Multidisciplinary characterization of the new species *Copemetopus mystakophoros* and its symbionts with a proposal for the new class Copemetopea (Alveolata: Ciliophora)

SERGEI I. FOKIN[1,2], VALENTINA SERRA[1,*], LEANDRO GAMMUTO[1], ALESSANDRO ALLIEVI[1], GIULIO PETRONI[1,3,4] and LETIZIA MODEO[1,3,4]

1 Department of Biology, University of Pisa, Pisa, Italy
2 Department of Invertebrate Zoology, St. Petersburg State University, St. Petersburg, Russia
3 CIME, Centro Interdipartimentale di Microscopia Elettronica, Università di Pisa, Pisa, Italy
4 CISUP, Centro per l'Integrazione della Strumentazione dell'Università di Pisa, Pisa, Italy

Abstract

The history of the genus *Copemetopus* is tortuous and studded with several misattributions. It was erected by Villeneuve-Brachon in 1940 after the discovery of *Copemetopus subsalsus* in saline ponds along the French coast of the Mediterranean Sea near Sète and associated with the class Heterotrichea in the family Metopidae, close to *Bryometopus*. After a long series of systematic revisions, it is now clear that *Copemetopus* is not a heterotrich and that it falls in the subphylum Intramacronucleata. Nevertheless, a lot more work is needed to fix the complex taxonomic status of the genus, which lacks a precise taxonomic collocation (it is presently referred to as *incertae sedis*). In the present study focused on a multidisciplinary and detailed description of a new species, of the genus, ***Copemetopus mystakophoros* sp. nov.**, we also propose the erection of the new class, **Copemetopea cl. nov.** After careful literature and data revision, we believe that members of *Copemetopus* require a higher-ranked taxon in the phylum Ciliophora, given their molecular and morphological peculiarities.

Keywords: 18S ribosomal DNA, brackish water, ecology, morphology, phylogeny, scanning electron microscopy, taxonomy, transmission electron microscopy

INTRODUCTION

Ciliates of the genus *Copemetopus* Villeneuve-Brachon, 1940 are protists of a large size that exhibit some obvious peculiar morphological characters. They are representatives of brackish or marine benthic biota and hypersaline aquatic communities. Besides, they have adapted to live in an almost anoxic environment. The genus was erected by Villeneuve-Brachon (1940) after the discovery of *Copemetopus subsalsus* Villeneuve-Brachon, 1940 in saline ponds along the French coast of the Mediterranean Sea near Sète, and was classified in the class Heterotrichea in the family Metopidae Kahl, 1927, close to *Bryometopus* Kahl, 1932. Because metopids are now included in the class Armophorea Lynn, 2004 and *Bryometopus* is a member of the class Colpodea Small & Lynn, 1981 (Foissner, 1993), it is obvious that this arrangement is no longer valid. However, *Copemetopus* was transferred without any explanation by Lynn (2008) from Metopidae to Condylostomatidae Kahl in Doflein & Reichenow, 1929, although this allocation can be dated back to Corliss (1979).

Until now, three species have been included officially in *Copemetopus* (i.e. *Copemetopus chesapeakensis* Small & Lynn, 1985, *Copemetopus subsalsus* and *Copemetopus verae* Campello-Nunes *et al.*, 2022). The first two species were treated in an extensive review of the taxonomy of the phylum Ciliophora by Jankowsky (2007) and placed in the family Climacostomidae Repak, 1972 (Heterotrichea), where *Copemetopus* had been included since 1985 (Small & Lynn, 1985).

*Corresponding author. E-mail: valentinasrr@gmail.com

The type species of *Copemetopus* is *C. subsalsus* designated by monotypy by Villeneuve-Brachon (1940). *Copemetopus verae* is the only species to have been investigated molecularly.

However, the history of the studies carried out on the genus is tortuous and studded with several misattributions. For example, *Copemetopus nasutus* (Da Cunha, 1915) was proposed by Esteban *et al.* (1995), but the species is instead *Metopus nasutus* Da Cunha, 1915 and does not possess any morphological features of *Copemetopus*. Another mistaken member of the genus, *Copemetopus simplex* Kahl, 1933, appears in the section dealing with the class Armophorea in the review by Jankowsky (2007: 525), who refers to the work where the ciliate was indicated as *Eometopus simplex* (Small & Lynn, 1985: 430). Moreover, *Copemetopus subsalsus* is also mentioned as being sampled in the Baltic Sea since 2001 by Mironova *et al.* (2009), although without any specific indication about the place where the species was retrieved and any morphological details. Considering that only pelagic ciliates were mentioned in that study, significant doubts can be expressed on the species attribution, because it seems unlikely that *Copemetopus* could have been sampled, given that it is a typical representative of brackish or marine benthic biota (Xu *et al.*, 2021). Likewise, the ciliate is also listed in the ciliate biodiversity dataset of the shallow Baltic Bay of Nivå, Denmark, in 2016 (https://www.gbif.org/occurrence/43991026) by the Department of Biology of the University of Copenhagen. In conclusion, in both the Baltic Sea cases, there is no certainty that the researchers discovered the same *Copemetopus* species as described by Villeneuve-Brachon (1940) from the Mediterranean.

Regarding *Copemetopus subsalsus*, after the first description by Villeneuve-Brachon (1940), a putative redescription was provided by Al-Rasheid (2001), but as discussed below, the obvious differences between the two studied species indicate that the two ciliates are not conspecific. Thus, the more recently described species will be referred to herein as *Copemetopus subsalsus sensu* Al-Rasheid (2001).

Until now, no molecular data have been available on *Copemetopus subsalsus*. Some transmission electron microscope (TEM) investigations were conducted on this species in the past (Iftode *et al.*, 1982; da Silva-Neto *et al.*, 1993) although they were published only as abstracts for meetings. No peer-reviewed paper has been published on the topic. Only recently, Campello-Nunes *et al.* (2022) presented under the name of *Copemetopus subsalsus* some TEM data and pictures provided by Dr F. Iftode who, in 1981, processed some specimens for electron microscopy from a sample collected in Île de Ré on the West Atlantic coast off France. As we discuss below, in our opinion several doubts should be expressed concerning the suitability of accepting these data as a supplement of the description by Villeneuve-Brachon (1940) of *Copemetopus subsalsus*.

Copemetopus chesapeakensis has been presented with only a single schematic image in both editions of the *Illustrated Guide to the Protozoa* (Small & Lynn, 1985: 438, Lynn & Small, 2002: 420), without any previous or further descriptions. Thus, it still constitutes an almost unknown species.

The most recently described species of the genus, *Copemetopus verae*, has been characterized through both morphological and molecular investigations. This study led to removal of *Copemetopus* from Heterotrichea (Campello-Nunes *et al.*, 2022).

During the years 2005–2008, we started our research on the genus *Copemetopus*. In that period, we were able repeatedly to collect representatives of a species of the genus from the brackish water pond situated on the coastline of the Ligurian Sea, close to the mouth of the Serchio River in the Pisa district, Tuscany, Italy. Unfortunately, at that time these ciliates could be presented only briefly (i.e. only a preliminary discussion concerning their morphology, ecology and possible

phylogenetical affiliation was provided; Fokin *et al*., 2006, 2008, 2009, 2019). In 2020, in samples from the marine lagoon of Orbetello along the Tyrrhenian coastline (Tuscany, Italy), we found another population of *Copemetopus* that was identical both morphologically and molecularly to the samples previously studied in our laboratory from the Serchio River. Thus, based on data collected from both the old and the new populations of the species, taking a multidisciplinary study approach (i.e. integrating molecular data with morphological ultrastructural observation) and performing a critical review of the literature, we had the chance to describe in full a new species of the genus, i.e. *Copemetopus mystakophoros*. We also took this opportunity to carry out a review of the phylogeny of the genus. Interestingly, not only did our research confirm the inaccuracy of the traditional view of *Copemetopus* as a heterotrich as recently proposed by Campello-Nunes *et al.*, (2022), but it also indicated the need to establish a new higher-ranked taxon dedicated to *Copemetopus* in the phylum Ciliophora.

MATERIAL AND METHODS

Sampling

The type population of the new species, *Copemetopus mystakophoros* (IPS3-1 population), was discovered in a brackish water pond (8–15‰ salinity) on the coastline of the Ligurian Sea, Pisa district (Tuscany, Italy), close to the mouth of the Serchio River (43°47′39″N, 10°16′4″E). Unfortunately, the type locality no longer exists because the pond where the species was found was destroyed by flooding of the Serchio River in 2009. Samples were taken at a depth between 30 cm and 1 m and contained water and part of the upper layer of bottom sediment. The first samples (IPS3-1, IPS3-2 and IPS3-3) were collected during October 2005, with a water temperature ranging from 18 to 22 °C. The salinity range and oxygen level were measured using an OX 22 oxygen meter (Aqualytic, Langen, Germany). The samples also contained other ciliates, such as *Sonderia vorax* Kahl, 1928, *Sonderia pharyngea* Kirby, 1934, *Plagiopyla* sp., *Condylostomides* sp., *Frontonia* sp. and *Metopus* sp., in low to moderate abundance. In the sediment layer, where *Copemetopus mystakophoros* was mainly discovered, the water oxygen level was 0.6–1.5%; in the water close to that sediment layer, the oxygen concentration was 1.0–6.8%, whereas close to the water surface it was 34–66%. The salinity of the samples was ~15‰.

Attempts to cultivate this *Copemetomus* population in the laboratory were unsuccessful in normal (oxygen) conditions. However, the ciliate survived in closed tubes in the original samples for a week and sometimes even longer. Thus, all investigations were performed on the specimens of the non-clonal type population from the original pond, taken from all three of the collected samples. The ciliate was collected repeatedly from the same brackish water pond in April 2006 in similar conditions and with the water temperature ranging from 14 to 16 °C, and in October 2006 with a water temperature 20 °C and salinity of 8‰.

The second population of *Copemetopus mystakophoros* (OALG11 population) was discovered in the north-west part of the marine lagoon of Orbetello, Laguna di Levante (34–46‰ salinity), located on the coastline of the Tyrrhenian Sea, Grosseto district (Tuscany, Italy; 42°27′08.8″N, 11°11′00.1″E) in July and October 2020 and in November 2021, with a water temperature of 24, 17 and 15 °C, respectively. The samples also contained other ciliates, such as *Metopus vestitus* Kahl, 1932, *Parablepharisma* sp., *Parablepharisma bacteriophora* Villeneuve-Brachon, 1940, *Gruberia* spp., *Plagiopyla* sp., *Euplotes* spp. and *Geleia* sp.

Live observations

Live ciliates were observed for morphological details using a differential interference contrast microscope with a Leitz (Weitzlar, Germany) instrument equipped with a digital camera (see below) at a magnification of ×300 to ×1250, with the help of a compression device (Skovorodkin,

1990). For examination of the swimming behaviour, the ciliates were observed in a glass depression slide (3 mL) under a dissection microscope (Wild M3, Switzerland) at a magnification of ×12.5 to ×50.0.

Fixation and staining

Ciliates were fixed with Champy's fluid, then impregnated with silver nitrate according to Corliss (1953). The Feulgen staining procedure after fixation in Bouin's fluid was used to reveal the nuclear apparatus. Some morphological observations of the ciliate were made after quick cell fixation (2–4 s) in 4% osmium tetroxide vapours.

Cell image capturing and measurements

Photomicrographs were captured from appropriate preparations with a digital camera (Canon PowerShot S45) and True Chrome HDII Screen, automatically saved as files during optical observation at a magnification of ×500 to ×1250 and used to obtain measurements of living and fixed ciliates. Schematic drawings, based on micrographs of typical living and silver nitrate-impregnated cells, were obtained by digitalizing pencil sketches on paper with the vector graphics program Inkscape v.0.92 (https://inkscape.org/); dotted lines were used to represent the inner cell structures.

Electron microscopy

Scanning electron microscope (SEM) preparations were obtained as described elsewhere (Modeo *et al.*, 2006), with some modifications. In particular, the fixation was performed using 2% osmium tetroxide in a solution of 0.1 M cacodylate buffer (pH 7.4) with 80% seawater. For the TEM, preparations were obtained according to either of the two following protocols: (1) fixation in 2.5% (v/v) glutaraldehyde in 0.1 M cacodylate buffer (pH 7.4), with a post-fixation in 1.5% osmium tetroxide in distilled water; then cells were processed through a routinely used protocol (Fokin & Görtz, 1993); or (2) fixation in a 1:1 mixture of 2.5% (v/v) glutaraldehyde in 0.1 M cacodylate buffer (pH 7.4) and 4% osmium tetroxide in distilled water; then cells were processed following Modeo *et al.* (2006).

Extraction of DNA and whole-genome amplification

Approximately 10–20 cells of *Copemetopus mystakophoros* IPS3-1 population were washed individually two or three times in sterile distilled water and fixed in 70% ethanol. Total genomic DNA extraction was performed using the NucleoSpin Plant II DNA extraction kit (Macherey-Nagel, Düren NRW, Germany).

Starting from around one or two cells of *Copemetopus mystakophoros* OALG11 population, the total DNA material was amplified via the whole-genome amplification (WGA) method, using the REPLI-g Single Cell Kit (QIAGEN, Hilden, Germany). In detail, we performed two WGA reactions, using two cells (OALG11_1) and one cell (OALG11_3), respectively. The cells were washed three times in distilled water and for a final time in phosphate-buffered saline (PBS). Then, they were transferred to a 0.2 mL Eppendorf tube together with 4 µL of PBS. The WGA protocol was completed following the manufacturer's instructions. The DNA material of OALG11_1 was processed with a Nextera XT library and sequenced at GENEWIZ Germany (Leipzig, Germany), using Illumina HiSeq X technology to generate 54 434 490 reads (paired ends, 2 × 150 bp). Preliminary assembly of the resulting reads was performed using SPAdes software (v.3.6.0) (Bankevich *et al.*, 2012). For the genomic analyses on *Copemetopus mystakophoros*, see the Supporting Information (Supplementary Text 1).

18S rDNA amplification and sequencing

Polymerase chain reactions (PCRs) were performed in a C1000 Thermal Cycler (Bio-Rad, Hercules, CA, USA). Almost the full length of the 18S rDNA sequence of *Copemetopus mystakophoros* was amplified from the total genomic extraction (IPS3-1) and from each WGA reaction (OALG11_1 and OALG11_3) using the following primer combination: 18S F9 (5′-CTGGTTGATCCTGCCAG-3′) (Medlin *et al.*, 1988) and 18S R1513 Hypo (5′-TGATCCTTCYGCAGGTTC-3′) (Petroni *et al.*, 2002). High-fidelity Takara Ex Taq PCR reagents were used (Takara Bio, Otsu, Japan) according to the manufacturer's protocol. The PCR cycles were set as follows: 3 min at 94 °C, 35 × (30 s at 94 °C, 30 s at 55 °C and 2 min at 72 °C) and 6 min at 72 °C. The PCR products were purified with the Eurogold Cycle-Pure Kit (EuroClone, Milan, Italy) and subsequently sent for direct sequencing to an external sequencing company, GENEWIZ Germany (Leipzig, Germany), by adding appropriate internal primers: 18S R536 (5′CTGGAATTACCGCGGCTG-3′), 18S R1052 (5′-AACTAAGAACGGCCATGCA-3′) and 18S F783 (5′-GACGATCAGATACCGTC-3′) (Rosati *et al.*, 2004).

Phylogenetic analyses

The three 18S rDNA sequences obtained from the two *Copemetopus mystakophoros* populations (IPS and OALG11) were aligned with the automatic aligner of the ARB software package v.5.5 (Westram *et al.*, 2011) on the SSU ref NR99 SILVA database (Quast *et al.*, 2013).

The identity matrix calculation was performed on selected representatives of the phylum Ciliophora (42 sequences).

For the phylogenetic analysis, our three sequences plus another 100 18S rDNA sequences belonging to representatives of the classes of Ciliophora were selected, for a total of 103 sequences (dataset 1).

In order to obtain more robust node support, a further three datasets were used to perform phylogenetic analyses. These three additional datasets were obtained by subsequent removals of sequences showing longer branches in our phylogenetic outputs. Therefore, starting from dataset 1, we obtained dataset 2 (92 sequences), dataset 3 (53 sequences) and dataset 4 (39 sequences). As an outgroup, we selected sequences belonging to subphylum Postciliodesmatophora.

After manual editing to optimize base pairing in the predicted rRNA stem regions in each dataset, the alignments were trimmed at both ends to the length of the shortest sequence. The resulting matrices contained 1199 (dataset 1), 1173 (dataset 2), 1137 (dataset 3) and 1121 (dataset 4) nucleotide positions, respectively.

For each phylogenetic dataset, the optimal substitution model was selected with jModelTest v.2.1 (Darriba *et al.*, 2011) according to the Akaike information criterion (AIC). Maximum likelihood (ML) trees were calculated with the software PHYML v.2.4 (Guindon & Gascuel, 2003) from the ARB package, performing 100 pseudoreplicates for all datasets. A Bayesian inference (BI) tree was inferred only for dataset 1 with MrBayes v.3.2 (Ronquist *et al.*, 2012), using three runs, each with one cold and three heated Markov chain Monte Carlo chains, with a burn-in of 25%, iterating for 4 500 000 generations.

Symbiont screening

Preliminary fluorescence *in situ* hybridization (FISH) experiments were performed on the IPS3-1 population, using the eubacterial generic probes EUB338I (Amann *et al.*, 1990) and ALF1b (Manz *et al.*, 1992), labelled with fluorescein isothiocyanate and cyanine-3 fluorophore, respectively. Specimens were fixed in 4% (v/v) formaldehyde in PBS. After the staining procedure, specimens

were observed under ultraviolet light with a fluorescent microscope Leica DMR (Leica, Switzerland) equipped with an Osram 50 W/AC L2 mercuric vapour lamp. Fixed cells were investigated simultaneously under ultraviolet light after staining with 4′,6-diamidino-2-phenylindole (DAPI) and ethidium bromide dyes.

Fluorescence *in situ* hybridization experiments could not be performed on OALG11 populations owing to the low number of cells retrieved in the sample.

Moreover, the presence of symbionts associated with *Copemetopus mystakophoros* was assessed through molecular analysis by means of two different methods: (1) via PCR with universal primers for the 16S rDNA of bacteria, cloning and sequencing (for the Serchio population, IPS3-1); and (2) via the 16S rDNA BLAST analysis on the genome assembly retrieved from the OALG11 population. The OALG11 strain preliminary assembly obtained from sequenced reads was inspected for the presence of 16S rDNA sequences using the software Barrnap v.0.5 (Seemann, 2013). The retrieved sequences were checked via blastn analysis on the NCBI blast web tool to obtain a preliminary taxonomic annotation. The 16S rDNAs were considered as belonging to possible symbionts only when present on contigs (i.e. sequences derived from the assembly of raw reads) with a coverage >100×; the excluded 16S rDNAs were classified as belonging to contaminants or to temporarily associated bacteria.

We used two different methods because the first analyses on *Copemetopus mystakophoros* (IPS3-1 population) were performed in 2008, and at that time, next generation sequencing (NGS) techniques were not available in our laboratory. Nomenclature of prokaryotes followed Oren & Garrity (2021).

RESULTS
SYSTEMATICS

Phylum Ciliophora Doflein, 1901
Subphylum Intramacronucleata Lynn, 1996
Class Copemetopea cl. nov.
Order Copemetopida ord. nov.
Family Copemetopidae fam. nov.
Genus *Copemetopus* Villeneuve-Brachon, 1940
Copemetopus mystakophoros sp. nov.
(Tables 1 and 2; Figs 1–12)

ZooBank registration (family) : urn:lsid:zoobank.org:act:8CCADA5A-654E-4DD3-BC78-03E733C1300E

Zoobank registration

(species) : urn:lsid:zoobank.org:act:D0B08C02-C63C-497A-A778-D3915329E63B

Diagnosis:

Size (all quantitative data are expressed as an average) *in vivo*, 275 µm × 120 µm; size after silver nitrate staining, 250 µm × 103 µm; cell generally resembling a club or a bowling pin in shape (i.e. presenting an expanded front end and an elongated rear end); oral aperture-to-body length ratio of 1:2.2. Macronucleus: usually in two equally elongated nodules, 41 µm × 24 µm in size and connected by a thin karyoplasmic isthmus. Micronuclei: 11, roundish, of the compact type, 3.8 µm in diameter. Contractile vacuole: single, in the posterior end of the cell, without collecting canals. Cytoplasmic features: invariably several hundreds of elongated symbiontophorous vacuoles (length, 6–8 µm) containing two types of bacteria [i.e. *Alphaproteobacteria* plus, probably (according to

morphology), spirochaetes]. Cortical granules: present, appearing as strips lying between the ciliary rows and consisting of three to five irregular rows of roundish granules each. Somatic kineties: 92; moustache (i.e. a row of long, whip-like ciliary units): 15 units, inserted on an outer border of the buccal cavity over the adoral zone of membranelles (AZM), without having any connection with it, and consisting of cilia with a length of up to half the cell length; dorsal brush (i.e. dense rows of longer somatic cilia beneath the anterior cell pole, on the right side): five or six rows; distinctive preoral suture. AZM: 45 membranelles; paroral membrane (PM): three ciliary rows, although sometimes not obvious. Swimming behaviour: ciliate, mainly rotating to the right and, less frequently, to the left direction. Habitat: brackish or marine water (salinity, 8–46‰), oxic–anoxic border in the bottom sediments.

Type locality:

The sampling site of the type population, IPS3-1, of *Copemetopus mystakophoros* was the permanent small brackish-water pond located along the Ligurian sea coastline close to the mouth of the Serchio River (Parco Naturale di Migliarino San Rossore Massaciuccoli, Migliarino, Pisa district, Tuscany, Italy (43°47′39″N, 10°16′4″E), sample no. 1 (IPS3-1); sampling date 16 October 2005; collector S. I. Fokin).

Type material:

One slide of the type population (IPS3-1) of *Copemetopus mystakophoros* with silver nitrate-impregnated holotype specimen (registration no. *CAMUS_2022-1*), indicated by a circle of ink on the coverslip, plus a paratype slide with permanent Feulgen-stained specimens (registration no. CAMUS_2022-2) have been deposited in the collection of the 'Museo di Storia Naturale e del Territorio dell'Università di Pisa' (Calci, Pisa, Italy).

Etymology:

The name is derived from Ancient Greek, μουστάκι (moustáki), meaning 'moustache', and from -phóros and -phoros, from the stem of φέρω (phérō), meaning 'to carry, bearing', because the species is characterized by long frontal ciliary whip-like units forming a sort of moustache inserted on an outer border of the buccal cavity over the adoral zone of the membranelles.

Voucher material:

The total genomic DNA of *Copemetopus mystakophoros* obtained from cells of the type population (IPS3-1) and the WGA products obtained from population OALG11 are available at the Department of Biology of the University of Pisa (Pisa, Italy), Unit of Zoology–Anthropology.

Gene sequences:

The 18S rDNA sequences of *Copemetopus mystakophoros* were deposited in NCBI GenBank database under the following accession numbers: OM955238 (from IPS3-1 population; 1773 bp long), OM955239 (from OALG11_1; 1738 bp long) and OM955240 (from OALG11_3; 1738 bp long).

Description:

Type population IPS3-1: Size of the ciliate variable, 200–450 μm × 90–150 μm *in vivo*; after fixation and silver staining, 188–328 μm × 78–135 μm (249.7 μm × 102.6 μm on average; Figs 1–4; Table 1). Length-to-width ratio close to 2.4:1 (Figs 1–6; Table 1). Cell size after SEM procedure: 100–205 μm × 65–135 μm (163 μm × 93.7 μm on average), with a cell shrinkage of 35% and 8.7% compared with *in vivo* length and width, respectively (Fig. 7). Cell shape elongated (oblong), sometimes ovoid, usually with an expanded cell anterior and a tapered posterior end; cell shape resembling a club (Figs 1–7A). Both cell ends rounded *in vivo* (Fig. 1). Shape changing from ovoid to club- (most commonly) or bowling pin-shaped observed in some cells in the population, possibly

as a consequence of the cell growing up process. Unfortunately, cell division and post-division processes were not observed. Generally, cells are spherical in cross-section, although most of the larger cells have a slight dorsoventrally flattened appearance.

Table 1. Morphometric data of *Copemetopus mystakophoros* sp. nov. type population

Character	Minimum	Maximum	Mean	SD	Coefficient of variation (%)	Number of cells
Body length	188	328	249.7	34.9	14.0	20
Body width	78	150	102.6	23.9	23.3	20
Body length*	100	205	163.7	55.9	34.2	3
Body width*	65	135	93.7	36.7	39.1	3
Oral aperture length	93	135	111.4	13.3	11.9	20
Oral aperture length/body length (%)	38	55	45.5	5.8	12.7	20
AZM, number of membranelles	42	48	44.6	1.9	4.3	15
Moustache, number of whip-like ciliary units	10	21	14.7	4.0	27.2	10
Somatic kineties, number	85	103	93.8	4.4	4.7	15
Somatic ciliature, number of cilia per unit	2	6	3.6	1.1	30.5	60
Macronucleus, number of pieces	2	2	2	0	0	15
Macronucleus, length of each piece	30.5	52	40.8	6.8	16.7	10
Macronucleus, width of each piece	18	30	24.0	3.8	15.8	10
Number of micronuclei	7	18	11.2	2.5	22.5	20
Micronucleus diameter	3	4	3.8	0.3	7.8	20

All data are based on silver nitrate-stained cells except for those indicated with an asterisk (*), which are from specimens processed for scanning electron microscopy, and data on the nuclear apparatus, which are based on Feulgen-stained cells. All measurements are in micrometres. Abbreviation: AZM, adoral zone of membranelles; SD, standard deviation.

Macronucleus (Ma) consisting of two oval nodules of equal size (41 μm × 24 μm in size each) connected by a thin karyoplasmic isthmus (Figs 1D, 2, 5, 8A, C); 11 roundish micronuclei (Mi; 3.8 μm in diameter) of the compact type distributed close or, sometimes, far from the Ma (Figs 2, 5; Tables 1 and 2; see below for ultrastructural details on nuclear apparatus).

A single large contractile vacuole (CV) with a single pore is located in the posterior end of the ciliate. Apparently, the CV pulsates with long breaks, hence its activity is difficult to detect (Figs 1E, 2). Cytoproct not visible.

In living conditions, many ciliates showed in the cytoplasm several relatively large food vacuoles (phagosomes) with a green content (Fig. 1A, B) and unknown cytoplasmic inclusions (Fig. 1E); neither bacteria nor diatoms were observed inside the phagosomes. In the cytoplasm, several hundreds of slightly elongated symbiontophorous vacuoles (SVs) were invariably observed (Fig. 8; see below for ultrastructural details).

The kinetome structure was visible in silver-stained ciliates and both in some living cells and in cells treated for FISH (see Fokin, 2016) thanks to the pattern of cortical granules (CGs). In FISH samples, the kinetome was mapped by strips highlighted by both *Eubacteria* and *Alphaprotobacteria* probes (Figs 3C, 6C) and consisted of CGs distributed in irregular rows (see below for ultrastructural details). According to FISH results, each strip consisted of between one and five CGs across, depending on the body region of the ciliate (Fig. 6C).

Table 2. Comparison of general morphological data of the different *Copemetopus* species

Species	Salinity (‰)	Size *in vivo* (µm)	Somatic kineties, number	AZM, number of membranelles	Somatic ciliature, number of cilia per unit	Moustache, number of whip-like ciliary units	Kinetosomal rows in DB, number	Mi, number	CV, position	Cortical granules, number in the strips	Mucocysts
Copemetopus subsalsus Villeneuve-Brachon, 1940	33?	300–400 × 100–125	90–100	32	?	9	?	8–10	Middle	2–3	+
Copemetopus subsalsus sensu Al-Rasheid (2001)*	130	200–400 × 65–130	70–102 (88)[a]	43–47 (44)	1[b]	9–10	6–7	9–15 (11)	Posterior	?	?
Copemetopus verae Capello-Nunes *et al.*, 2022	17	120–208 × 43–85	60–88 (72)	31–44 (37)	2–4[c]	10[d]	6–11 (8)	2–17 (7)	–	–	–
Copemetopus chesapeakensis Small & Lynn, 1985	nd	nd	nd	35[e]	nd	19[e]	nd	3[e]	nd	nd	nd
Copemetopus mystakophoros Present study (type population)	15	200–450 × 90–150	85–103 (92)	42–48 (45)	2–6 (4)	8–21 (15)	5–6	7–18 (11)	Posterior	3–5	–

*Published as *Copemetopus subsalsus* (Al-Rasheid, 2001; see main text for details);
[a]arithmetic means;
[b]reported in the text but, according to figs 18–23, p. 192 (Al-Rasheid, 2001), in each ciliary unit there are two or even three cilia;
[c]number reported in the text only;
[d]number reported only according to Fig. 4C;
[e]data according to illustration.
Abbreviations: AZM, adoral zone of membranelles; CV, contractile vacuole; DB, dorsal brush; Ma, macronucleus; Mi, micronucleus; nd, no data; Ref., reference; ?, uncertain description; +, character present; –, character not present.

Somatic cilia were ~10 µm long *in vivo*; caudal cilia were not detected (Figs 1, 2, 7). Somatic cilia units were ciliferous on both ventral and dorsal sides of the cell, mainly consisting of three or four cilia (3.6 on average in line), but with unit composition ranging between two (dikinetids), five and six (polykinetids) in the set (see below for ultrastructural details; Figs 7, 9–11; Table 2). No special ciliary fields with an identical organization to most of such units were observed (Figs 4, 7). Somatic ciliary rows: ~85–103 (93.8 on average; Table 1).

A single row of long, whip-like ciliary units, forming a sort of moustache, is present at the anterior region of the oral cavity near to AZM on its outer perimeter. The moustache (number of whip-like ciliary units, 10–21; 15 on average) is located along the membranelles of AZM, but independent from them (Figs 1C–F, 2, 3D, E, 4C, 7, 9A, B); at their own base (SEM width, ~2.8 µm), moustache units consisted of a combination of two or three tightly located layers of eight to ten rows of long cilia (Figs 7, 9A, B). Moustache extends up to half of the body of the ciliate (i.e. 100–150 µm), with units becoming thinner from their insertion to the tip (Figs 2, 7, 9A, B) and clearly not participating in AZM beating activity, but performing one or more different functions yet to be elucidated. Some living cells in calm conditions (i.e. without movement) repeatedly showed a fan-like or nimbus-like moustache position with respect to the cell body (Figs 1E, 2), whereas during movement they showed a ‘folded’ moustache (i.e. located in parallel along the body; Fig. 1C).

The preoral suture is conspicuous, presenting an empty space and running from the upper right side of the buccal aperture almost to the right anterior part of the cell dorsal side (Fig. 7). On the dorsal side, part of five or six kinetosome rows beneath the anterior pole on the right side consisting of closely located sets of kinetosomes, the so-called dorsal bristle. Cilia of the region are longer (~15–20 µm *in vivo*) than the rest of the dorsal somatic kineties cilia, therefore forming a kind of tuft, clearly visible in living cells and in some fixed cells (Figs 1A, 3B, 4A, 7).

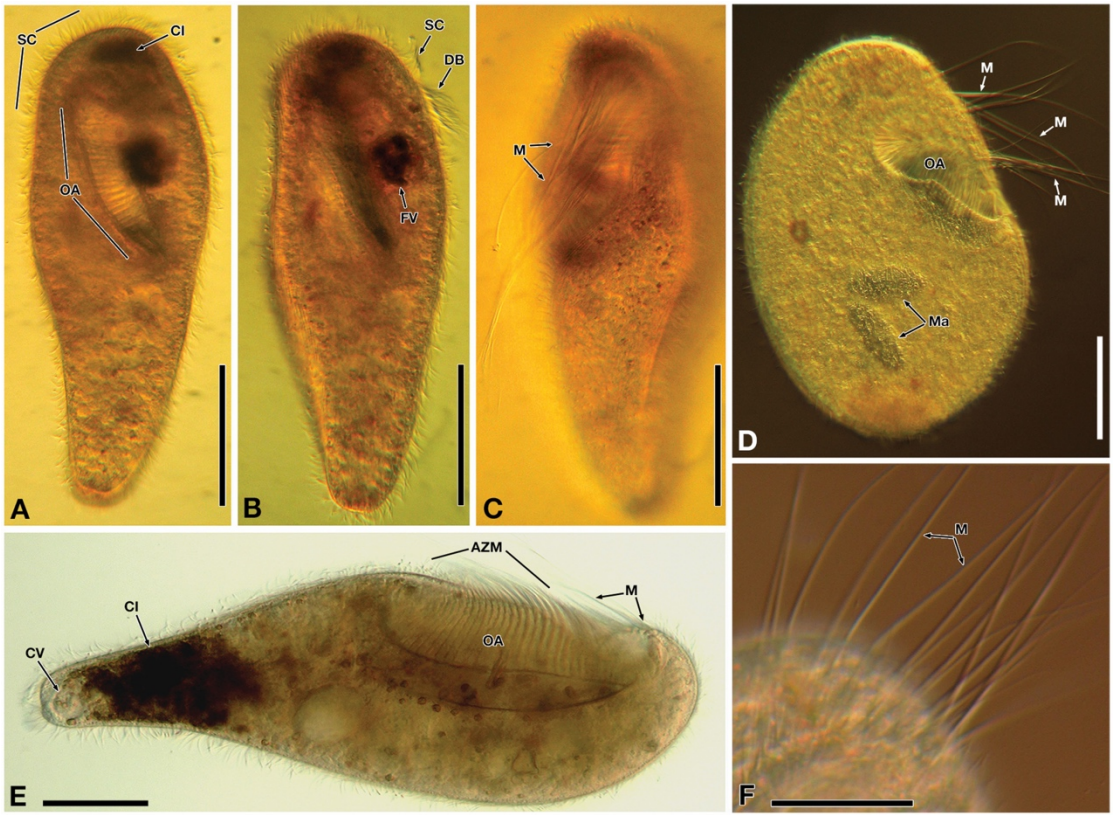

Figure 1. General view of *Copemetopus mystakophoros* sp. nov. based on micrographs of living cells using a differential interference contrast microscope. A–C, the same living cell, with the typical elongated (oblong) shape, from the dorsal (A, B) and ventral (C) view. D, E, living cells in lateral view: D, view of a specimen with a roundish shape; E, view of a cell with an enormously large oral aperture. F, cell anterior region when the moustache has a fan-like position. Abbreviations: AZM, adoral zone of membranelles; CI, cytoplasmic inclusions; CV, contractile vacuole; DB, dorsal brush; FV, food vacuole; M, moustache; Ma, macronucleus; OA, oral aperture; SC, somatic cilia. Scale bars: 70 µm in A–C; 80 µm in D; 50 µm in E; 60 µm in F.

Length of the oral aperture reaching almost half of the body length (45.5% on average, based on silver nitrate-stained specimens); oral aperture oval-elongated, usually oblique, with a slightly expanded frontal part located along the middle axis of the ventral side of the ciliate and a narrowed rear part lying closer to its right edge with an angle of ~20° (Figs 1, 3, 4, 7). Oral aperture always positioned close to the frontal edge of the cell, but with an inclination with respect to the cell longitudinal axis sometimes higher (i.e. ≤50°). Paroral membrane consisting of three closely located rows (not always very distinct from each other) of short cilia (length, ~6 µm *in vivo*; Figs 2, 3D, E, 4B, C, 7) running on the right side of the oral cavity. Distinct whirling S-shaped AZM, with 42–48 membranelles (44.6 on average), occupying the left side of the oral groove (Figs 1E, 2, 3C, D, 4C, 7).

Ultrastructural features:

Rod-shaped bacterial ectosymbionts can sometimes be detected on the cell surface in living and fixed ciliates, both after staining with DAPI dye (Fig. 6A, B) and after the TEM procedure (Fig. 10A); in TEM sections, ectosymbionts are tangentially and perpendicularly oriented with respect to the cell surface. The SEM investigation did not show any ectosymbiotic bacteria on the cell surface, possibly for technical reasons connected to the SEM procedure performed (Figs 7, 9).

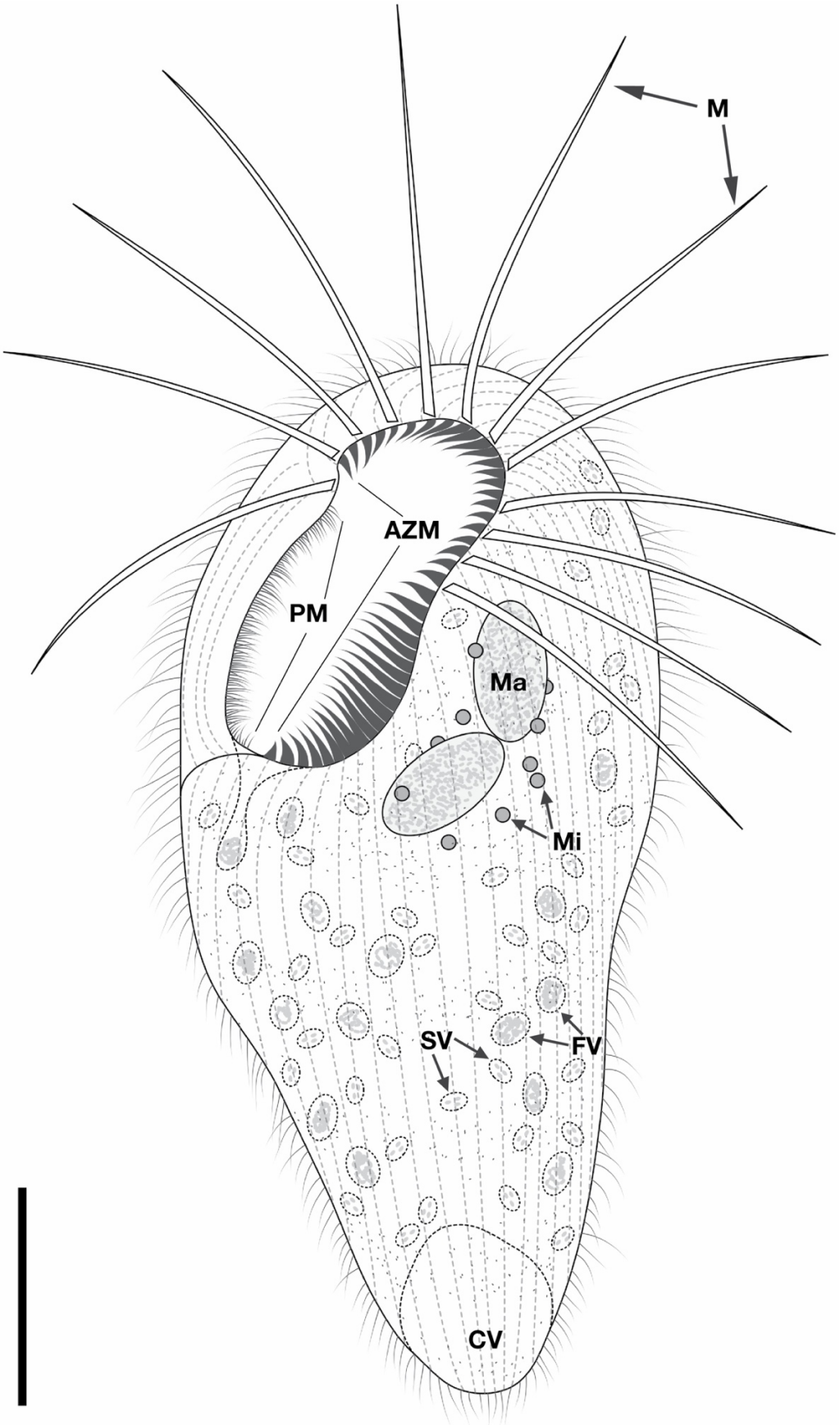

Figure 2. Schematic drawing to illustrate the general shape and morphological characteristics of *Copemetopus mystakophoros* sp. nov. in ventral view, based on micrographs of living and silver nitrate-stained cells. Abbreviations: AZM, adoral zone of membranelles; CV, contractile vacuole; FV, food vacuole; M, moustache; Ma, macronucleus; Mi, micronuclei; PM, paroral membrane; SV, symbiontophorous vacuoles. Scale bar: 50 µm.

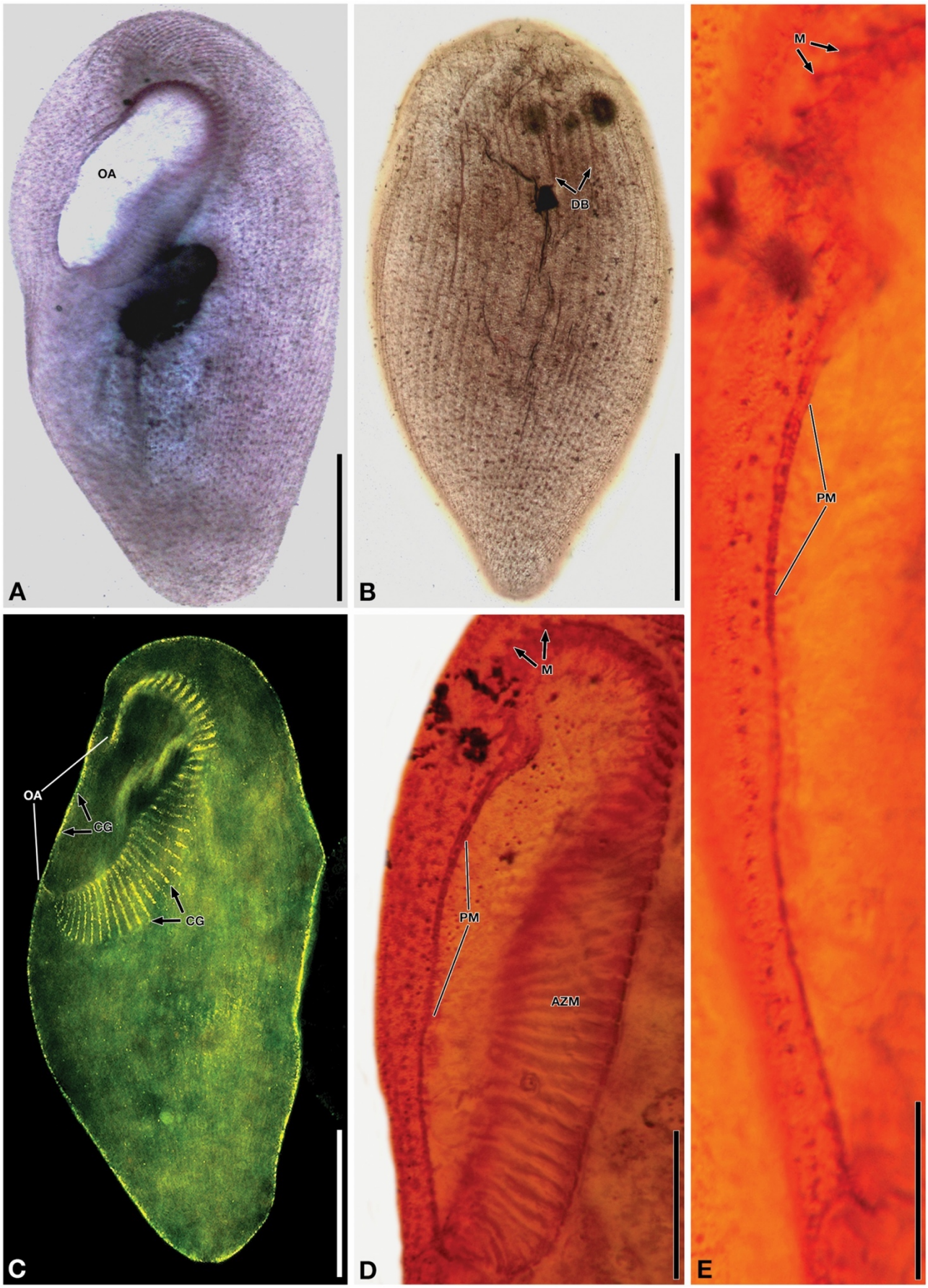

Figure 3. Cells of *Copemetopus mystakophoros* sp. nov. after impregnation by silver nitrate (A, B, D, E) and after FISH reaction (C). Abbreviations: AZM, adoral zone of membranelles; CG, cortical granules; DB, dorsal brush; M, moustache; OA, oral aperture; PM, paroral membrane. Scale bars: 80 μm in A–C; 25 μm in D; 16 μm in E.

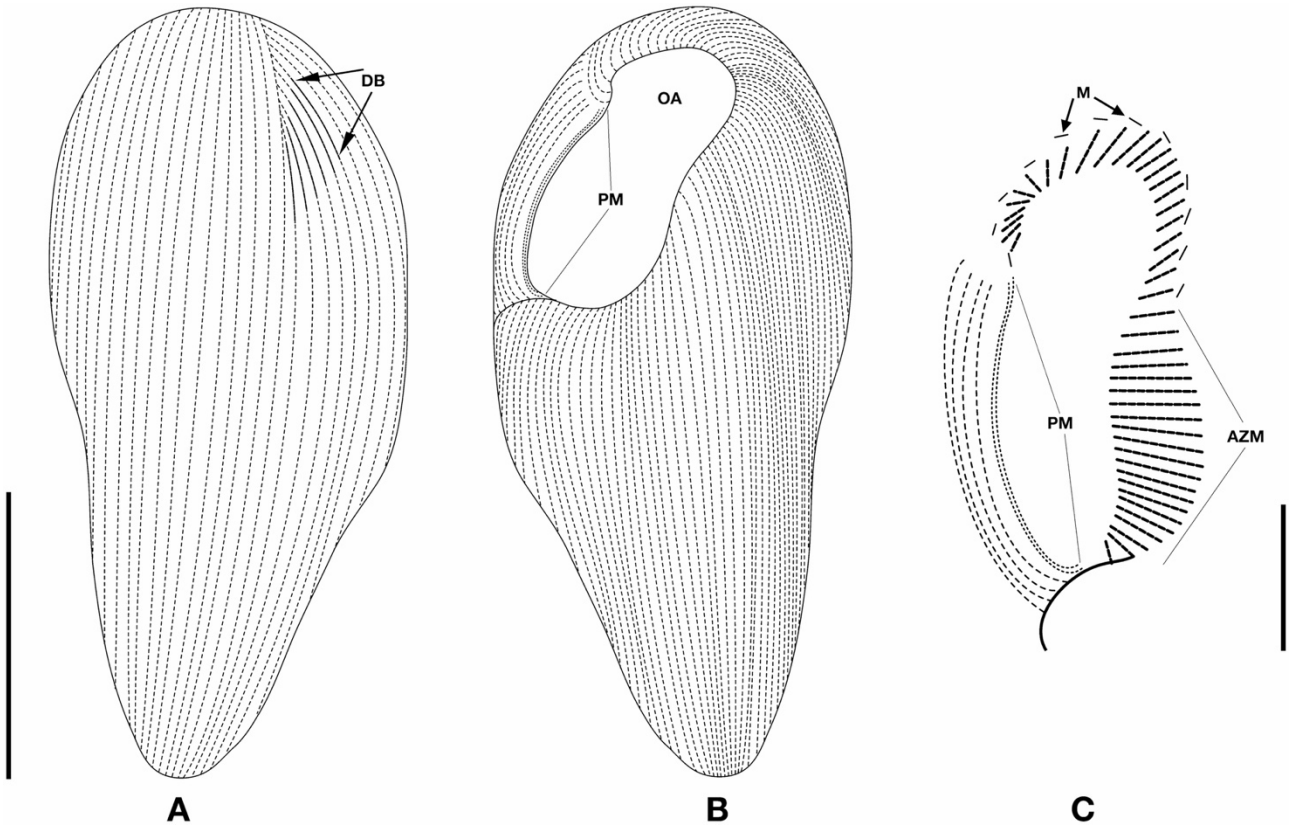

Figure 4. Schematic drawing to illustrate the dorsal and the ventral somatic ciliature of *Copemetopus mystakophoros* sp. nov. (A, B) and the organization of the oral region ciliature (C) based on silver-impregnated cells. Abbreviations: AZM, adoral zone of membranelles; DB, dorsal brush; M, moustache; OA, oral aperture; PM, paroral membrane. Scale bars: 100 μm in A, B; 35 μm in C.

In the cortex: (1) under the plasma membrane, flat alveoli and many non-homogeneous, roundish to slightly elongated to even irregularly shaped CGs (length, ~0.5–0.8 μm) sprout in a single, irregular layer (more commonly) but are sometimes distributed in several layers (Figs 6C, 10A, B, E–G); and (2) regarding the somatic infraciliature, both dikinetids (Figs 10A–C, 11) and polykinetids (Fig. 10D, E) were observed and their ultrastructure investigated in both cross-section (Fig. 10C, D, F) and longitudinal section (Fig. 10A, E). Electron-dense material surrounds the somatic dikinetids and forms a desmose linking the two kinetosomes to each other; from the desmose, a roundish spur of electron-dense material arises anterior to the left (Fig. 10C). As for the fibrillar associates, the anterior kinetosome shows a tangential ribbon consisting of six or seven transverse microtubules plus, in front of triplet 4, an isolated couple of additional microtubules with an apparently perpendicular orientation with respect to the tangential ribbon; the posterior kinetosome shows a striated kinetodesmal fibre (Fig. 10C, F, G) oriented towards the right or slightly posteriad and contacting the anterior kinetosome; an electron-dense structure arises posteriad to the right, with between six and 15 long postciliary microtubules curving posteriad and forming flat ribbons; no stacking of the ribbons was observed (i.e. postciliodesma were not detected; Fig. 10F, G). In between kinetosomes, there are no additional microtubules (Fig. 10C). In polykinetids, such as triplets of kinetosomes, the anteriormost and posteriormost kinetosomes do not diverge from corresponding kinetosomes in dikinetids; the middle-located kinetosome presents transverse microtubules and is linked by a desmose to the posterior one (Fig. 10D). Along the kinetosomes, longitudinal microtubules, underlined by a microfibrillar network system, run in parallel (Fig. 10A, E, F).

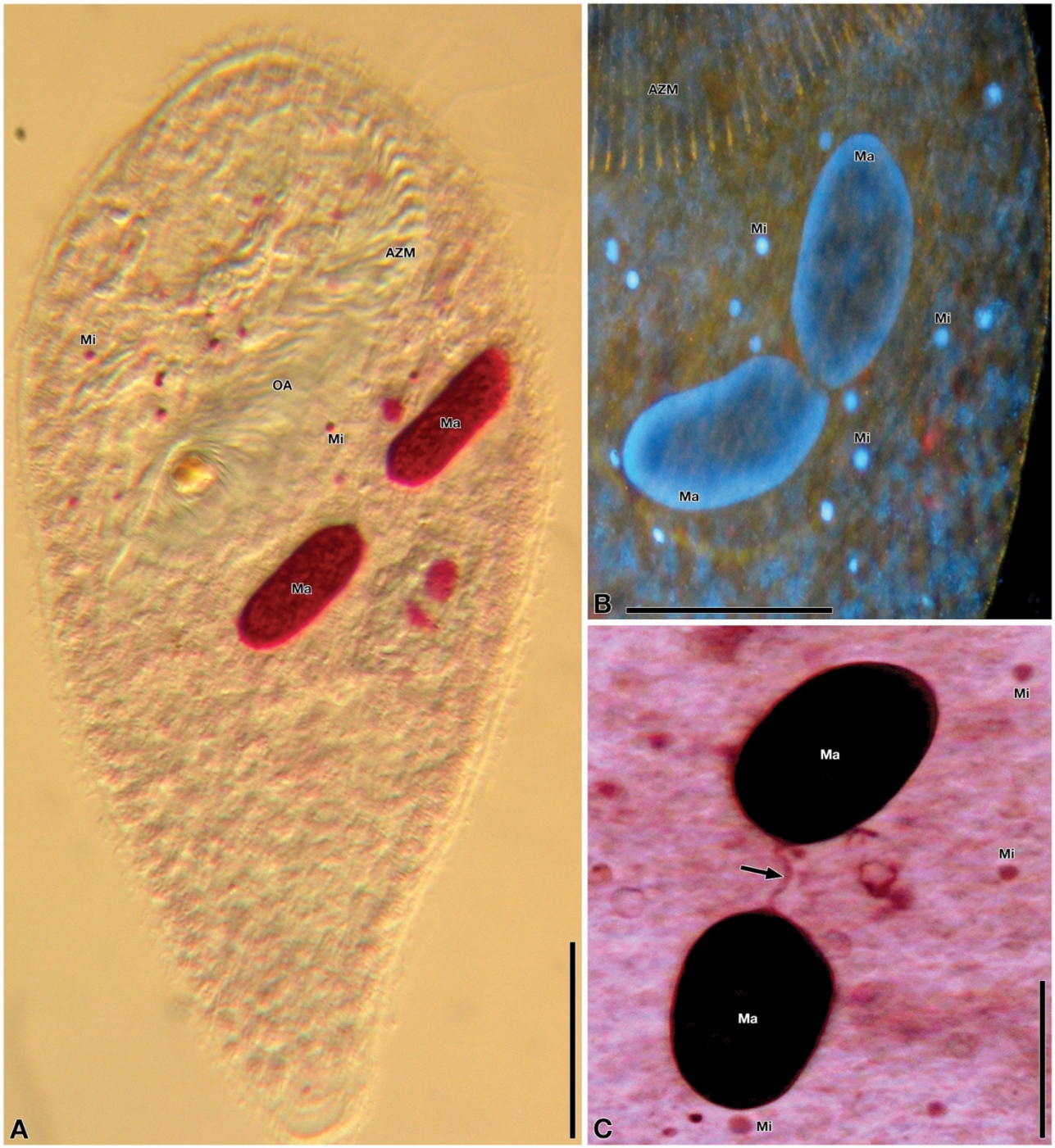

Figure 5. A, C, nuclear apparatus of *Copemetopus mystakophoros* sp. nov. in cells stained by the Feulgen method (A, C) and 4′,6-diamidino-2-phenylindole (DAPI) (B). C, two macronuclear nodules are linked by a thin karyoplasmic isthmus (arrow). Abbreviations: AZM, adoral zone of membranelles; Ma, macronucleus; Mi, micronucleus; OA, oral aperture. Scale bars: 50 µm in A; 40 µm in B; 35 µm in C.

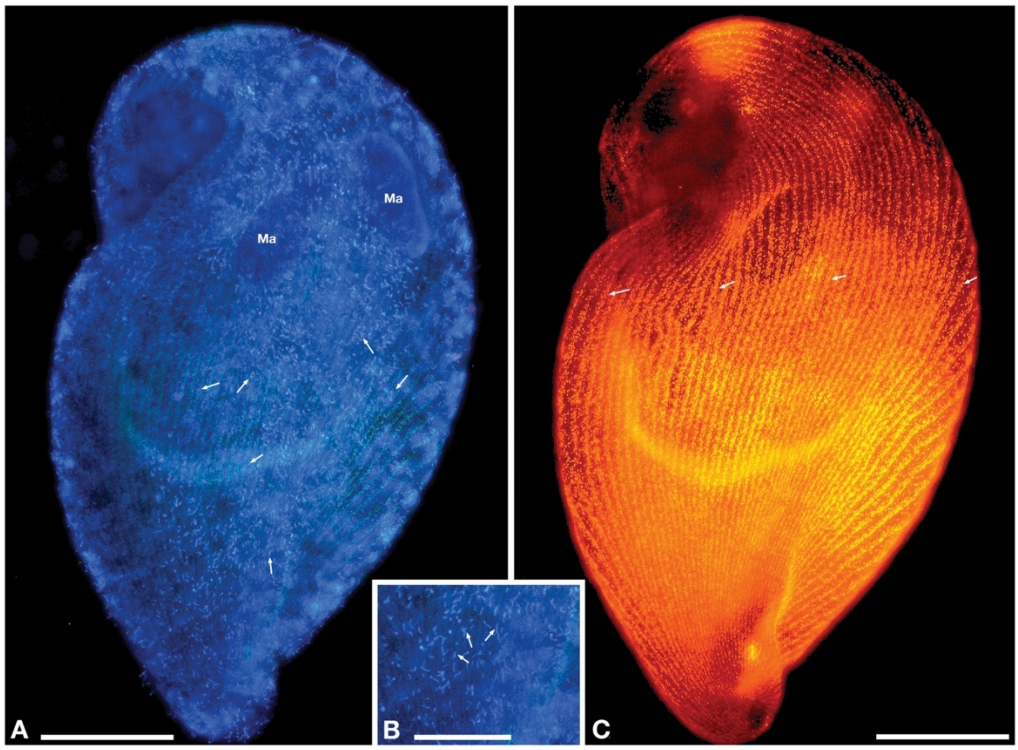

Figure 6. General morphology of a *Copemetopus mystakophoros* sp. nov. specimen in lateral view after 4′,6-diamidino-2-phenylindole (DAPI) staining and fluorescence *in situ* hybridization (FISH) experiment. A, B, same fixed ciliate after DAPI staining at lower (A) and higher (B) magnification. In B, the ectosymbionts (arrows) are clearly visible lying on the cell surface. C, FISH experiment showing a peculiar arrangement of the cortical granules (arrows); the probe signal is not related to the presence of ectosymbionts. Abbreviation: Ma, macronucleus. Scale bars: 60 µm in A, C; 30 µm in B.

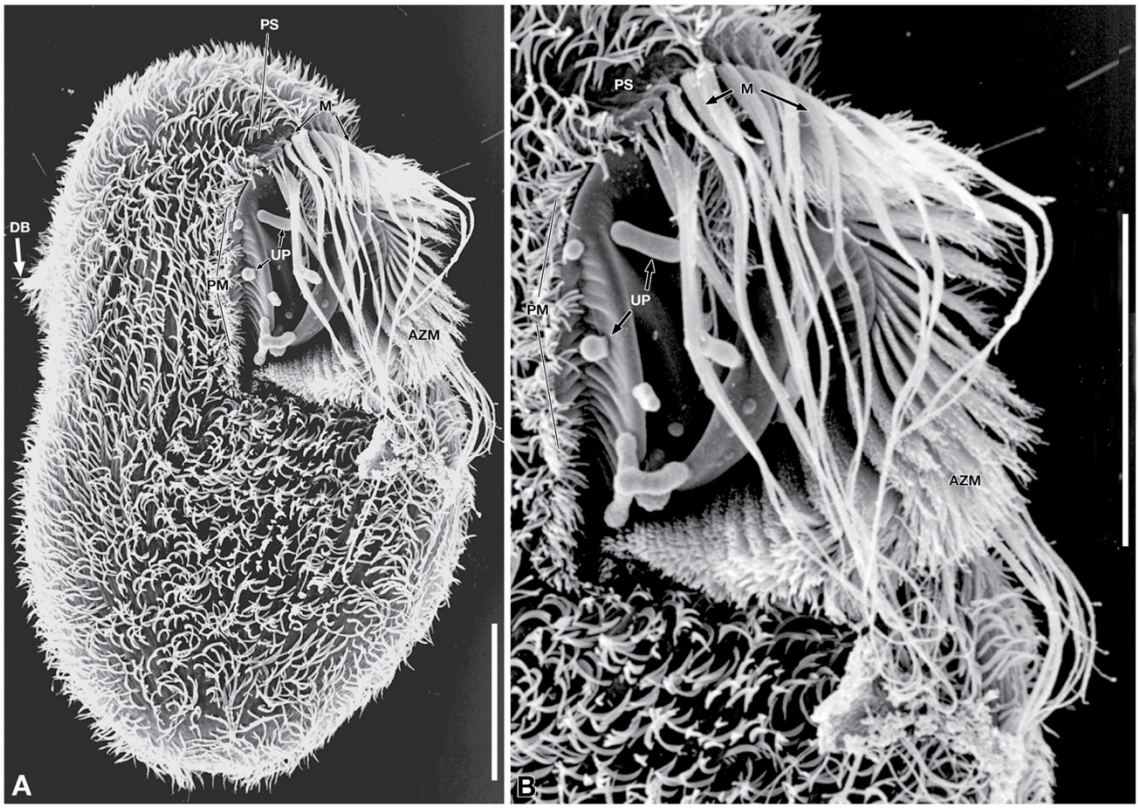

Figure 7. *Copemetopus mystakophoros* sp. nov. viewed under the scanning electron microscope. A, general view of a specimen from the lateral side. B, oral area at higher magnification. Abbreviations: AZM, adoral zone of membranelles; DB, dorsal brush; M, moustache; PM, paroral membrane; PS, preoral suture; UP, unknown particles sticking to the buccal cavity surface. Scale bars: 70 µm.

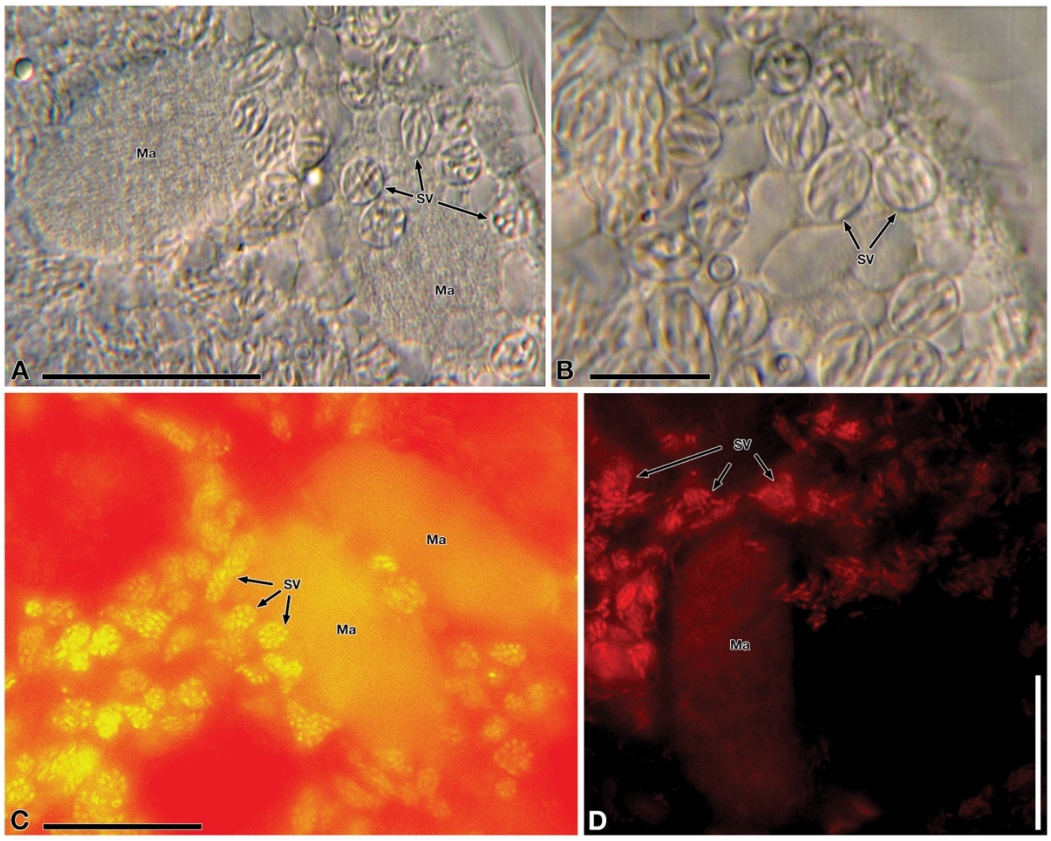

Figure 8. Cytoplasmic symbionts in the symbiontophorous vacuoles in living (A, B) and stained (C, D) cells of *Copemetopus mystakophoros* sp. nov. A, B, differential interference contrast microscope images showing prokaryotic symbionts. C, ethidium bromide staining to highlight the presence of symbionts. D, fluorescence *in situ* hybridization experiment, with the fluorescent probe ALF1b showing a positive signal (emitting in red). Abbreviations: Ma, macronucleus; SV, symbiontophorous vacuole. Scale bars: 45 µm in A; 12 µm in B; 35 µm in C, D.

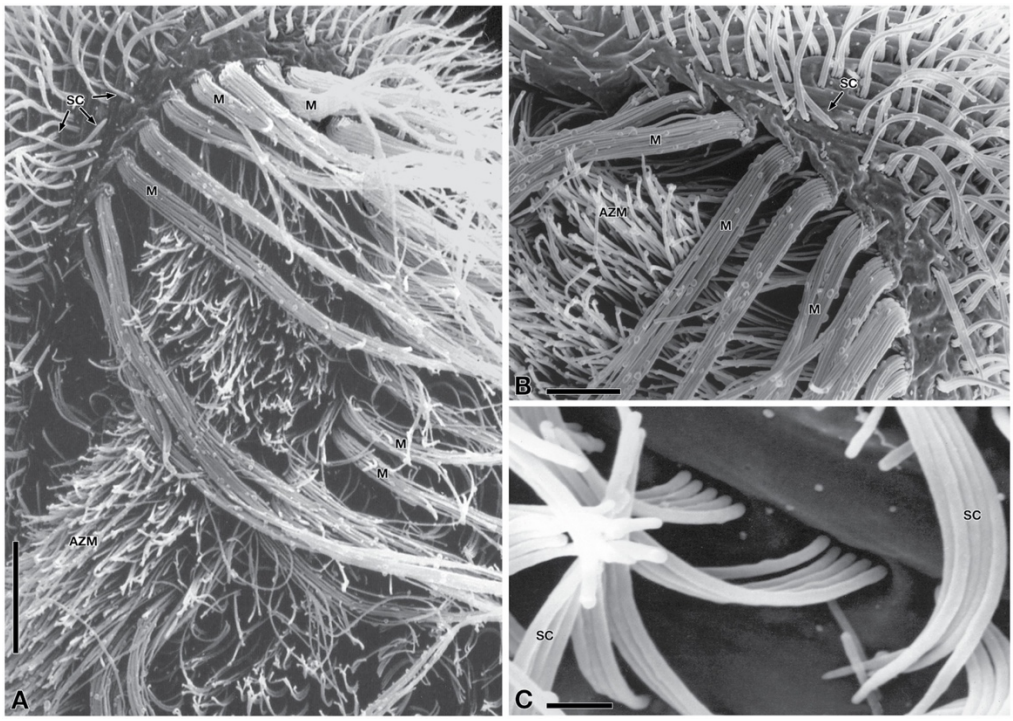

Figure 9. Details of *Copemetopus mystakophoros* sp. nov. viewed under the scanning electron microscope. A, B, structure of the moustache, consisting of whip-like ciliary units. Abbreviations: AZM, adoral zone of membranelles; M, moustache; SC, somatic cilia. Scale bars: 15 µm in A; 10 µm in B; 1 µm in C.

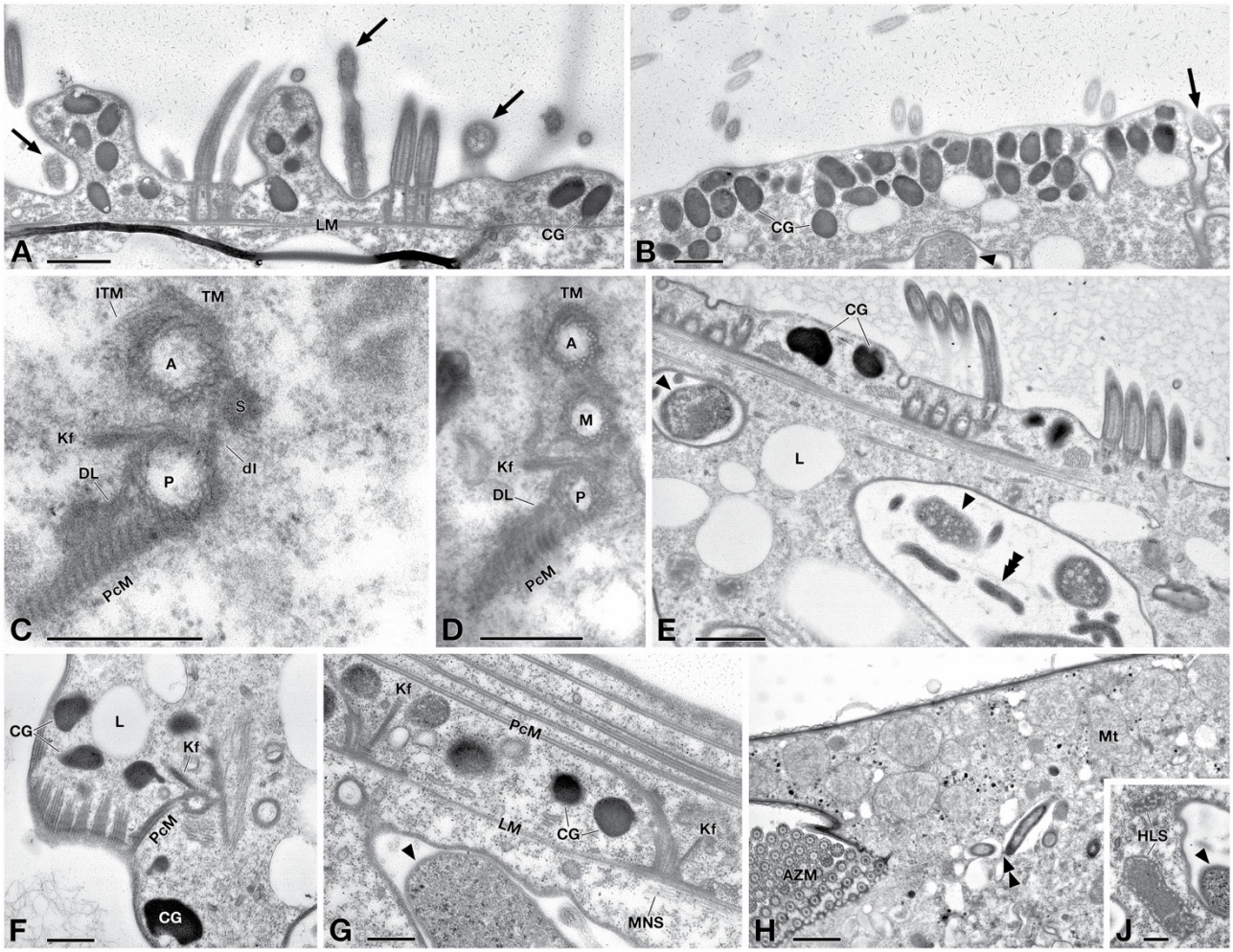

Figure 10. Details of the cortex of *Copemetopus mystakophoros* sp. nov. viewed under the transmission electron microscope. A, C–G, infraciliature topology and root structures associated with kinetosomes. Cortical granules can be seen in A, B, E, F, G. H, classical mitochondria are present in the oral region of the ciliate, with hydrogenosome-like structures diffusely present in the rest of the cytoplasm (J). Dikinetids are shown in longitudinal section (A, B) and cross-section (C, F, G); polykinetids in cross-section (D) and longitudinal section (E). Arrows indicate ectobacteria. In symbiontophorous vacuoles: arrowheads indicate *Pseudomonadota* bacteria, whereas triple arrowheads indicate spirochaete-like bacteria. Double arrowheads point to another type of cytoplasmic bacteria. Abbreviations: A, anterior kinetosome; AZM, adoral zone of membranelles; CG, cortical granules; dI, desmose of electron-dense material linking the two kinetosomes to each other; DL, dense lamina; HLS, hydrogenosome-like structures; ITM, isolated microtubules departing from anterior kinetosome; Kf, kinetodesmal fibre; L, lipid droplets; LM, longitudinal microtubules; Mk, middle-located kinetosome; MNS, microfibrillar network system; Mt, mitochondria; P, posterior kinetosome; PcM, postciliary microtubules; S, roundish spur of electron-dense material; TM, transverse microtubules. Scale bars: 1 μm in A, B, E, H; 0.5 μm in C, D, F, G, J.

In the cytoplasm:

1. There are a huge number of medium-sized to large lipid droplets (Figs 10E, F, 12A, C).
2. Invariably, there are several hundreds of slightly elongated SVs (6–8 μm in length; Fig. 8) containing two types of bacteria: type I, elongated rod-shaped bacteria, 3.0–3.5 μm × 1.0–1.2 μm in size; and type II, twisted bacteria, 2.0–3.0 μm × 0.15–0.20 μm in size (Fig. 12A, B). According to FISH analysis, type I, targeted by the ALF1b probe, is a representative of *Pseudomonadota* (Fig. 8D); according to their general morphology and shape, type II are probably spirochaetes (Fig. 12A, B). Both bacterial types do not manifest distinctive nucleoids. Within each SV, there are usually around ten representatives of each bacterial type present simultaneously; SVs are often in contact with the rough endoplasmic reticulum cisternae of the ciliate (Fig. 12A, B). On a few sections, a third type of rod-shaped

cytoplasmic bacteria within individual vacuoles can be observed near the ciliate cortex layer (Fig. 10H).

3. The nodules of Ma show dense chromatin bodies and several nucleoli, whereas Mi contain a less packed chromatin (Fig. 12C, D).
4. There are two types of energy-related organelles: in the oral cavity region, closer to the cell surface, there are classical mitochondria, with a size of 1.5 μm × 2.0 μm and tubular cristae (Fig. 10H); and more deeply in the ciliate cytoplasm, among the SVs, there are many hydrogenosome-like organelles (1.2 μm × 0.6 μm), with a homogeneous, more electron-dense core (matrix) surrounded by several peripheral tubular–vesicular (swollen) cristae-like structures (Figs 10J, 12A, B).

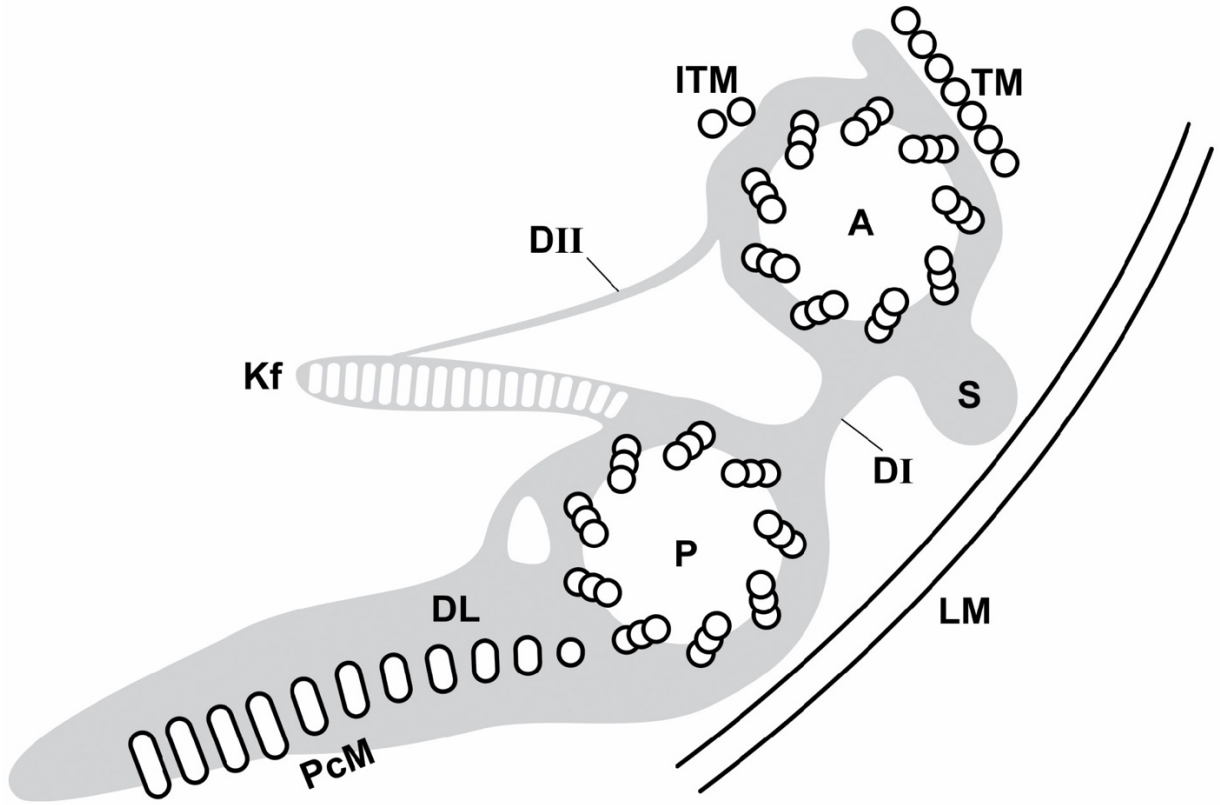

Figure 11. Schematic diagram of the somatic dikinetid of *Copemetopus mystakophoros* sp. nov. based on transmission electron microscopic observation. Abbreviations: A, anterior kinetosome; DI, desmose of electron-dense material linking the two kinetosomes to each other; DII, desmose of electron-dense material linking the anterior kinetosome to the kinetodesmal fibre; DL, dense lamina; ITM, isolated microtubules departing from anterior kinetosome; Kf, kinetodesmal fibre; LM, longitudinal microtubules; P, posterior kinetosome; PcM, postciliary microtubules; S, roundish spur of electron-dense material; TM, transverse microtubules.

Notes on biology and ecology:

The ciliate was observed near the bottom of the water bodies, in the water–sediment interface or even in the upper loose layer of bottom sediments. All samples containing *Copemetopus mystakophoros* smelled strongly of hydrogen sulfide. The oxygen level in water of this sediment layer varied between 0.6 and 1.1%. During the collection of living cells from the native sample into the depression slide in the laboratory, oxygenation was not tolerated by *Copemetopus mystakophoros* cells, which disappeared in <1 h. In contrast, the change of salinity conditions turned out not to be critical for survival of the ciliate when salinity remained at least in a brackish range or increased to 60‰. During most of the previous ciliate study period in our laboratory (i.e. 2005–2008), the salinity of the water in the sampling place remained within the brackish water range (8–15‰). Unfortunately, in 2008, after a severe storm and flood in the Serchio River mouth coastline, the ecology of the water reservoir, where representatives of *Copemetopus mystakophoros*

had been collected previously, was completely destroyed. The salinity decreased to almost zero, and the entire set of characteristic ciliate species in the bottom layer disappeared. However, during the recent study period (2020–2021), the water in the collecting place (i.e. the Laguna di Levante in Orbetello) always showed a higher salinity (34, 36, 39 and even 46‰) with a significant presence of hydrogen sulfide, indicating that these sampling conditions are suitable to sustain the survival of *Copemetopus mystakophoros*.

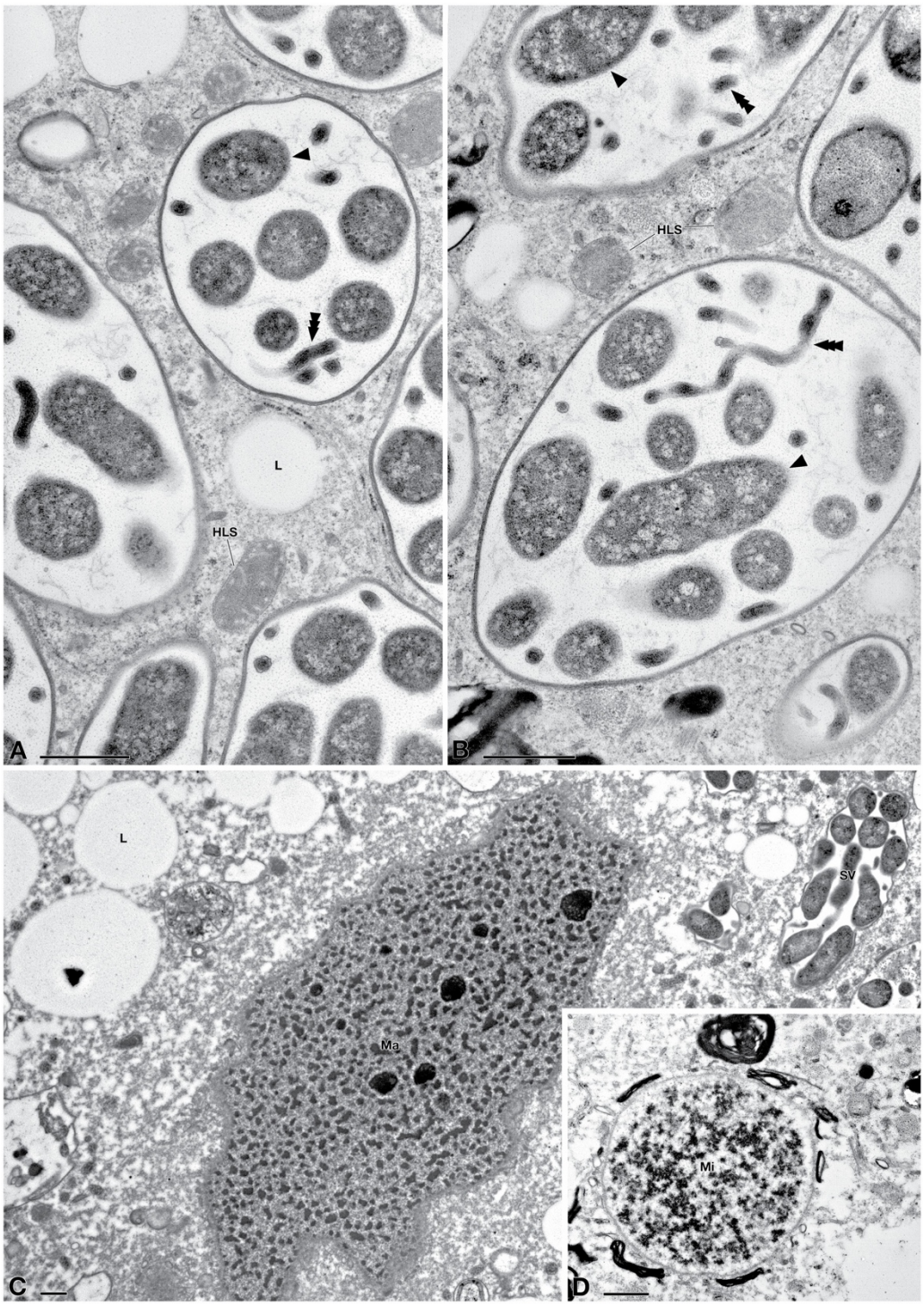

Figure 12. Details of *Copemetopus mystakophoros* sp. nov. viewed under the transmission electron microscope. A, B, cytoplasmic symbiontophorous vacuoles containing two types of bacteria. C, D, the nuclear apparatus: macronucleus and micronucleus. Arrowhead indicates *Pseudomonadota* bacteria, and triple arrowhead indicates spirochaete-like bacteria. Abbreviations: HLS, hydrogenosome-like structures; L, lipid droplets; Ma, macronucleus; Mi, micronucleus. Scale bars: 1 μm.

The swimming rotation of the ciliate was in a clockwise direction with respect to the longitudinal body axis, viewed from the posterior end. In a few cases, an anticlockwise direction was also observed.

It is noteworthy that during the entire study we have not been able to detect any dividing cell of the ciliate. However, this also applies to the other ciliate representatives of this ecological station studied in parallel, such as *Metopus*, *Parablepharisma*, *Plagiopyla* and *Sonderia*.

Marine or brackish water samples, according to our observations, are more stable than freshwater ones, and the ecological succession of organisms in the former (should it occur) usually proceeds more slowly than in the latter samples. Apparently, *Copemetopus mystakophoros* can survive adverse conditions by forming cysts. Repeated checks of the samples taken from Laguna di Levante, Orbetello, showed that the ciliate disappeared in the native/original samples a few days after the opening of the Falcon tubes in the laboratory (in July 2020 and November 2021), appearing again after 3–4 months in the same samples kept in closed conditions, but disappearing again a few days later.

Molecular and phylogenetic analysis

The three obtained 18S rDNA sequences of *Copemetopus mystakophoros* (IPS3-1, OALG111 and OALG11-3) were substantially identical except for one nucleotide in position 639 of the type sequence (IPS3-1). In this position, each electropherogram of *Copemetopus mystakophoros* from Orbetello presented a double peak, always involving A and G, which we interpreted as a polymorphism of the species.

The BLAST search on NCBI of the IPS3-1 *Copemetopus mystakophoros* sequence gave the following best hits: *Copemetopus verae* MZ441076 and MZ441075, showing 98.39 and 98.37% identity, respectively (23 mismatches, three or four gaps); three 'uncultured eukaryotes/ciliates', KT346288, KJ760065 and KT346292, showing 88.66, 88.62 and 88.52% identity, respectively; and *Parablepharisma bacteriophora* (MN319554) and *Meseres corlissi* Petz & Foissner, 1992 (EU399528) showing 88.53 and 88.35% identity, respectively.

From the identity matrix (Supporting Information, Table S1), the average identity of *Copemetopus* species with selected representatives of the phylum Ciliophora was 83.78%.

In our phylogenetic tree (Fig. 13), sequences of *Copemetopus mystakophoros* clustered together with those of *Copemetopus verae* with high statistical support (BI/ML: 0.97/99), showing that they represent two different *Copemetopus* species. Moreover, in all our phylogenetic analyses the *Copemetopus mystakophoros* sequences clustered together inside the Intramacronucleata clade, branching basally to the Armophorea–Litostomatea–Odontostomatea–Cariacotrichea–Muranotrichea–Spirotrichea group (Fig. 13; Supporting Information, Figs S1–S3).

As an additional sister group to the *Copemetopus* clade, besides the other aforementioned classes, there was the Protocruziea clade. All the other Intramacronucleata [(Plagiopylea, Prostomatea, Oligohymenophorea, Colpodea) and (Phyllopharingea, Nassophorea)] formed a sister group to them all (Fig. 13).

Statistical values were often not sufficiently robust in our analysis, especially for dataset 1 (Fig. 13), probably owing to the presence of different evolutionary rates among ciliate clades (e.g. Odontostomatea, *Licnophora*) that determine long branches in the phylogenetic tree. For this reason, we performed extra analyses using reduced databases (databases 2–4), which provided more

robust statistical support, especially for the nodes involving *Copemetopus* sequences: 36, 49 and 86% of bootstrap, respectively (Supporting Information, Figs S1–S3).

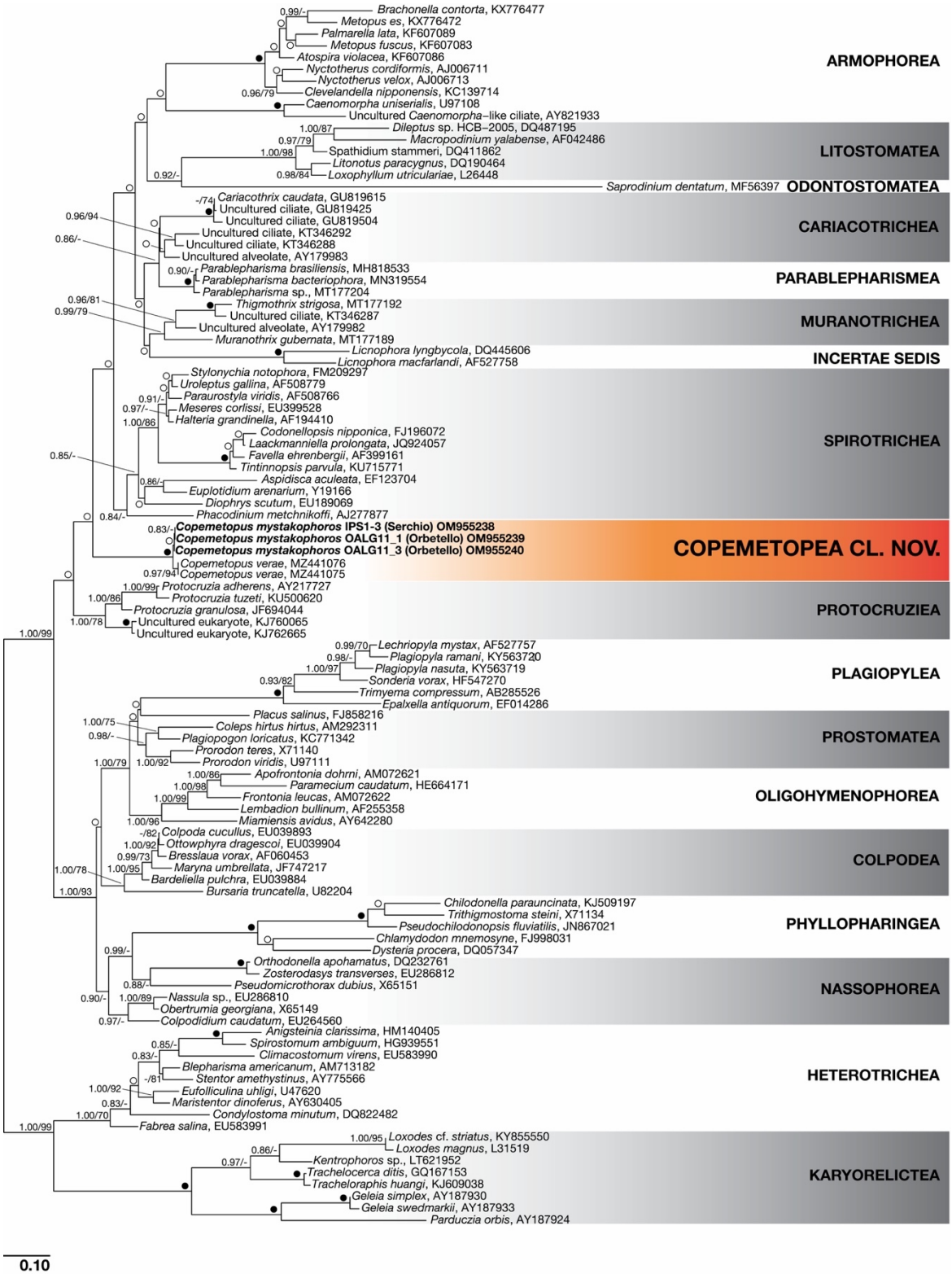

Figure 13. Maximum likelihood tree of the phylum Ciliophora based on 18S rDNA sequences (dataset 1). The phylogenetic relationships of *Copemetopus mystakophoros* sp. nov. are shown. Numbers associated with nodes represent the posterior probabilities from Bayesian inference (BI) and bootstrap values from maximum likelihood (ML) analyses, respectively (only values of BI ≥ 0.80 and ML ≥ 70% are shown). Black dots represent the highest statistical support (BI = 1.00 and ML = 100); white dots indicate non-significant statistical support (BI < 0.80 and ML < 70%). Sequences obtained in the present work are in bold.

Screening of the symbionts

Preliminary FISH results showed positive signals in response to the ALF1b probe (Fig. 8D) and to ethidium bromide (Fig. 8C) in the symbiontophorous vacuoles of IPS3-1 cells. Staining with DAPI also highlighted the presence of prokaryotes associated with the ciliates' cell surface (Fig. 6A, B).

From the screening performed on the IPS3-1 population using molecular methods, we retrieved two 16S rDNA consensus sequences, operational taxonomic unit (OTU) #1 and #2 (Table 3). From NGS methods on the OALG11 population, we retrieved another four sequences, OTUs #3–#6 (Table 3). All the 16S rDNA sequences obtained in the present work were deposited in NCBI GenBank database, under the accession numbers given in Table 3.

Table 3. 16S rDNA sequences of prokaryotes associated with *Copemetopus mystakophoros* sp. nov.

OTU	From	Length (bp)	Method	Coverage	Accession number	Best BLAST hits	Identity (%)	Systematics
#1	IPS3-1 (Serchio)	1500	PCR/cloning	–	OM959542	Uncultured bacterium clone G4_10.3_2, FJ717262	87.47	*Bacteria*, *Planctomycetota*, *incertae sedis*
						Uncultured bacterium clone SYNH02_C3-07B-128, JQ245570	98.28	
#2	IPS3-1 (Serchio)	1493	PCR/cloning	–	OM959543	Spirochete endosymbiont of a lucinid bivalve, AM236337	94.02	*Bacteria, Spirochaetota*
						Marispirochaeta aestuarii strain JC444, NR_158116.1	89.72	
#3	OALG11_1 (Orbetello)	1127	NGS	6.7×	OM959544	Uncultured crenarchaeote clone, EU732005	98.04	*Archaea, Crenarchaeota,* Asgard group
						'*Candidatus* Lokiarchaeota archaeon', MW958504	97.80	
#4	OALG11_1 (Orbetello)	732	NGS	1466.94×	OM959545	Bacterium enrichment culture clone Tol_54, HQ622276	100	*Bacteria, Thermodesulfobacteriota; Desulfobacterales*
						Desulfotignum sp. strain 4S-PR-S3-s2, MG264264	97.97	
#5	OALG11_1 (Orbetello)	1598	NGS	395.71×	OM959546	Uncultured bacterium clone T3-1_203, KX097725	87.18	*Bacteria*, FCB group; *'Candidatus* Cloacimonetes'
						'*Candidatus* Cloacamonas acidaminovorans', CU466930	82.67	
#6	OALG11_1 (Orbetello)	1515	NGS	25.4×	OM959547	*Arcobacter butzleri*, LC574939	94.82	*Bacteria, Campylobacterota, Campylobacterales*

Abbreviations: NGS, next generation sequencing; PCR, polymerase chain reaction.

We found six different 16S rDNA sequences, belonging to different bacterial classes and even bacterial phyla and domains: a bacterium belonging to a still undescribed clade related to *Planctomycetota* (*incertae sedis*, *Bacteria*: *Planctomycetota*), OTU #1, and a spirochaete bacterium (*Bacteria*: *Spirochaetota*), OTU #2, in the IPS3-1 population; and in the OALG11 population we found members of the following: (1) Asgard group (*Archaea*: *Crenarchaeota*), OTU #3; (2) *Desulfobacterales* (*Bacteria*: *Thermodesulfobacteriota*), OTU #4; (3) '*Candidatus* Cloacimonetes' [*Fibrobacteres–Chlorobi–Bacteroidetes* (FCB) group; *Bacteria*], OTU #5; and (4) *Campylobacterales* (*Bacteria*: *Campylobacterota*), OTU #6. The results of the BLAST analyses on the retrieved sequences are shown in detail in Table 3.

Testing *in silico* to compare the retrieved 16S rDNA from the IPS3-1 population with the oligonucleotide sequence of ALF1 probe showed only a partial matching in both the OTUs (seven nucleotides for OTU #1; seven to nine nucleotides for OTU #2, out of 17).

DISCUSSION

Copemetopus mystakophoros: a new member of the genus

The analysis of the morphology of the investigated ciliate gives reason to consider it as a new species of the genus *Copemetopus*. The most distinctive features of the genus are the usually relatively large cell sizes, 200–450 μm × 65–150 μm in live conditions (Table 2), and the usually club- or bowling pin-like shape of the body, expanded anteriorly and elongated posteriorly. Additional noticeable morphological characters are as follows: (1) a Ma consisting of two slightly elongated nodules, equally sized, connected by a karyoplasmic isthmus; (2) a constantly high number of Mi (usually between eight and 18); (3) an oral groove occupying almost half of the cell body; and (4) besides the classical AZM membranelles, the presence of a moustache, formed by not less than eight whip-like ciliary units and located along the outer edge of the AZM, but not directly associated with it (Tables 1 and 2).

The combination of these features in our species with several others (i.e. the number of cilia per somatic ciliary unit, the number of moustache whip-like ciliary units, the position of the CV, the arrangement of the CGs and the presence of mucocysts, a preoral suture and cytoplasmic endosymbionts), which do not agree between *Copemetopus mystakophoros* and *Copemetopus subsalsus* according to the original description of the latter (Villeneuve-Brachon, 1940), supports their separation (for details, see Table 2). Moreover, several important features of *Copemetopus mystakophoros* (i.e. the number of cilia per somatic ciliary unit and of ciliary rows in the dorsal bristle, the number of moustache whip-like ciliary units and the presence of CGs and endosymbionts) distinguish the species from *Copemetopus subsalsus sensu* Al-Rasheid (2001) [for details, see Table 2; for a discussion on the possible conspecificity of *Copemetopus subsalsus* Villeneuve-Brachon, 1940, and *Copemetopus subsalsus sensu* Al-Rasheid (2001), see below]. According to the only available material (i.e. a single schematic drawing, in which only 35 membranelles of AZM, 19 whip-like ciliary units in the moustache, plus three Mi are illustrated by Small & Lynn, 1985), *Copemetopus chesapeakensis* might possibly constitute an additional, independent species of the genus, but at present, due to the lack of reliable morphological data, the comparison with *Copemetopus mystakophoros* is meant to be extremely preliminary (Table 2). Indeed, should someone succeed in finding *Copemetopus chesapeakensis* in nature again, a thorough investigation of this ciliate is recommended, principally to support the species validity. Finally, the comparison with the last described species of the genus (i.e. *Copemetopus verae*; Campello-Nunes *et al.*, 2022) showed that *Copemetopus mystakophoros* and *Copemetopus verae* clearly differ in many morphological traits, such as their size, the number of their somatic kineties, cilia per somatic ciliary unit and ciliary rows in the dorsal bristle, the number of moustache whip-like ciliary units and the presence of the CV and the CGs (for details, see Table 2). Also, the presence of cytoplasmic endosymbionts in *Copemetopus mystakophoros* constitutes a clear morphological difference. Moreover, the identity among their 18S rDNA sequences suggests that *Copemetopus mystakophoros* and *Copemetopus verae* are two different species, confirming morphological data. Therefore, we think that we are dealing with a new morphological species of the genus.

However, concerning the presence of endosymbionts in the cytoplasm, which appears obvious in *Copemetopus mystakophoros* and constitutes an important diagnostic character according to the modern species description criteria (Serra *et al.*, 2020), it cannot be excluded *a priori* that they were possibly overlooked by previous researchers of *Copemetopus* spp., and the symbiontophorous vacuoles were considered as digestive vacuoles. Definitely, an investigation of the ciliate subcellular morphology would have been of great help.

In this regard, it should be highlighted that the present study is the first to adopt a multidisciplinary approach to study a *Copemetopus* species in depth, concurrently providing morphological and

ultrastructural data by means of SEM and TEM, combined with molecular phylogenetic analysis. Campello-Nunes *et al.* (2022) recently published a study of the morphology of *Copemetopus verae* by light microscopy and SEM combined with 18S rDNA sequencing but did not provide a TEM description of the species. Moreover, in the same paper, they presented a TEM study of another *Copemetopus* species, which they stated to be *Copemetopus subsalsus* Villeneuve-Brachon, 1940 although only a few pictures of barely five protargol-stained cells were provided. Additionally, a comparison with the original description of the ciliate was not possible, owing to the lack of a morphometric table. A significant part of the illustrative material of the article (three of nine figures devoted to morphology) deals with the study of the ultrathin structure of this putative *Copemetopus subsalsus* sampled, identified and processed for TEM in 1981 by the French protistologist Dr F. Iftode, who provided Campello-Nunes and colleagues with material. The sample originated from Île de Ré, an island off the West Atlantic coast of France, thus from a site located far from the Mediterranean Sea, where *Copemetopus subsalsus* was first found and described by Dr S. Villeneuve-Brachon in 1940. That being the case, and considering the recommendations from previous literature concerning the relevance of biogeography during species attribution (Warren *et al.*, 2017; Agatha *et al.*, 2021), we express our concern about the opportunity and the correctness of accepting this TEM investigation as a supplement to the work of 1940. However, it is worth noting, that, according to the published TEM pictures, several details of the composition of the somatic kinetosomes and their derivatives, in addition to the cytoplasmic decoration of nuclei (at least the micronuclei) and a peculiar appearance of the energy-related organelles, are common traits between the 'Atlantic' *Copemetopus* and *Copemetopus mystakophoros*. Nevertheless, the energy-related organelles, referred to as mitochondria in the former species (see Campello-Nunes *et al.*, 2022: fig. 10F, H), should be considered hydrogenosome-like structures, as in *Copemetopus mystakophoros* (Campello-Nunes *et al.*, 2022: fig. 10J) they appear obviously different from the typical mitochondria observed concurrently in the ciliate cytoplasm (Campello-Nunes *et al.*, 2022: fig. 10H). Moreover, figure 6B, F in the paper by Campello-Nunes *et al.* (2022) shows that the 'Atlantic' *Copemetopus* contains cytoplasmic vacuoles with an obvious double set of symbiotic bacteria, recalling those observed in the present study in *Copemetopus mystakophoros* (Figs 10B, E, G, 12A–C), which unfortunately, have been completely untreated by these authors.

The morphological comparison between the characteristics of *Copemetopus subsalsus* according to the original description (Villeneuve-Brachon, 1940) and the subsequent putative redescription (Al-Rasheid, 2001) reveals many incongruencies (Table 2), primarily concerning the position and shape of the CV (middle body *vs.* posterior), the mucocysts (present vs. supposed, although not clearly identified in the cell by the author, Al-Rasheid, 2001), the occurrence and arrangement of the CGs (two or three granules per row vs. it is not clear whether the character is present or can be identified as such) and the dorsal brush of cilia (not clear whether the character is present or can be identified as such vs. six or seven kinetosome rows). Even the macronuclear shape differs between the two studied ciliates. This situation clearly indicates that the two researchers dealt with two different species. Therefore, the redescription made in 2001 should be recognized as non-valid, and the ciliate redescribed should be treated as a separate species of the genus, which should be better (at least at present) referred to as *Copemetopus subsalsus sensu* Al-Rasheid (2001).

All the authors who previously studied species of the genus *Copemetopus* in detail (i.e. Villeneuve-Brachon, 1940; Al-Rasheid, 2001; Campello-Nunes *et al.*, 2022) did not investigate in depth the organization and function of the moustache. For instance, they did not notice that the moustache ciliary units are a combination of long cilia not associated with AZM, with a different function not directly related to the feeding activity of the ciliate. We believe that although the surface structures of the ciliate were investigated with modern techniques, such as SEM (Al-Rasheid, 2001: figs 18–23; Campello-Nunes *et al.*, 2022: fig. 4A–D), this misinterpretation might also be attributable to the non-optimal quality of the SEM images obtained, because, based on our own direct experience in

the field, classical SEM protocols are not easily adapted to the preservation requirements of *Copemetopus* cells. Additionally, our observations on living cells indicate that the moustache does not have the classical beating activity of somatic cilia and AZM membranelles. The cilia of the moustache can move apart only in the form of a fan (corolla) when the ciliate stops moving and thereby help in stabilizing the position of the cell among the particles of the bottom detritus. This activity recalls a kind of levitation (soaring) and, possibly, could be considered as part of a special type of feeding behaviour. When the ciliate is moving, the moustache is placed passively as a bundle along the cell body.

The presence of both classical mitochondria and hydrogenosome-like organelles is a peculiarity of *Copemetopus mystakophoros*. To the best of our knowledge, this situation has never been described before. At present, we do not have a satisfactory explanation for this phenomenon. From an evolutionary point of view, however, the presence of two forms of energy-related organelles in organisms living at the oxic–anoxic interface would be justified, also considering that in another *Copemetopus* species (i.e. *Copemetopus verae*) that is able to survive only in anaerobic conditions, only a single type of organelle (probably hydrogenosomes, according to the authors) have been reported (Campello-Nunes *et al.*, 2022).

The observed variability in size and shape of the cells of *Copemetopus mystakophoros* and even the configuration of its oral aperture could be associated with the different cell cycle stages. However, we could not yet observe the dividing process of the ciliate, and this has also been reported for *Copemetopus verae* (Campello-Nunes *et al.*, 2022). This might possibly be attributable to some influence of the oxygen-free habitat on the ciliate life cycle, because we observed the same feature (i.e. the lack of dividing forms in the population) for all the other ciliate representatives of the same ecological group as *Copemetopus mystakophoros*, which we sampled concurrently and, in some cases, investigated, namely *Metopus*, *Sonderia*, *Plagiopyla* and *Parablepharisma* (Esteban *et al.*, 1995; Modeo *et al.*, 2013; Nitla *et al.*, 2019; Campello-Nunes *et al.*, 2020). Unfortunately, at present we cannot offer a plausible explanation for this phenomenon, which deserves future investigation.

Another interesting feature observed in *Copemetopus mystakophoros* is the abundant presence of CGs, although their function in this context is unknown. Some ciliates show the presence of coloured (i.e. the pigmentocysts) or colourless CGs as a category of extrusive organelles. They are especially common in ciliates of the class Heterotrichea, where they are involved in several functions (Lynn & Corliss, 1991; Rosati & Modeo, 2003; Lynn, 2008; Buonanno & Ortenzi, 2018), but they are also present in representatives of some other classes, such as Armophorea, Karyorelictea, Nassophorea, Plagiopylea and Spirotrichea (for example, see Lynn 2008; Fokin, 2016). Thus, this feature is not useful for class assignment of a genus. However, their arrangement can be considered important both for the description of the species and, as discussed above, for the comparison with congenerics. Cortical granules are usually arranged in a single layer, forming longitudinal strips between kinetids of the ciliates. Often, each of these strips has its own design (i.e. the order and number of CGs in the strip; Boscaro *et al.*, 2014; Fokin, 2016). In the case of *Copemetopus mystakophoros*, the organization of a layer of these structures does not have a definite design, and from time to time they can form two layers. In a strip, they do not form accurate rows, but they are located chaotically, and in different parts of the cell body the strips formed can be narrower or wider (see Fig. 10A, B, E–G). *Copemetopus subsalsus* has a similar design of CGs, but each strip is bordered by two lines of mucocysts, which have not been reported in any of the other described *Copemetopus* species (Al-Rasheid, 2001; Campello-Nunes *et al.*, 2022) or observed in our *Copemetopus mystakophoros* (Table 2). However, in the case of the Arabian *Copemetopus* population, the anterior region of the cell is darkened due to yellowish-brown subpellicular granules (Al-Rasheid, 2001; Table 2).

The unique combination of the features of *Copemetopus mystakophoros* supports the proposal of a new class Copemetopea

The molecular and phylogenetic analyses clearly showed that the gene sequences of *Copemetopus* do not cluster with any other ciliate class, being basal to the clade formed by Spirotrichea–Armophorea–Litostomatea (the so-called SAL clade). The SAL clade also includes the recently established Cariacotrichea (Orsi *et al.*, 2012), Muranotrichea, Parablepharismea (Rotterová *et al.*, 2020) and Odontostomatea (Fernandes *et al.*, 2018) in the subphylum Intramacronucleata (Fig. 13).

Our phylogenetic analysis is coherent with that presented by Campello-Nunes *et al.* (2022). The only exception concerns the sequences of *Copemetopus verae* clustering as a sister group to *Protocruzia*, whereas in our analysis the class Protocruziea is basal to all the other classes in the clade (Copemetopea included). This discrepancy is probably attributable to the high instability of the groups under study and does not arouse particular surprise or concern.

Therefore, our analysis agrees with Campello-Nunes *et al.* (2022) in disproving the affiliation of *Copemetopus* to the class Heterotrichea, to which it was previously assigned (Villeneuve-Brachon, 1940; Al-Rasheid, 2001). Not by chance, beyond an apparent resemblance, *Copemetopus* possesses the following distinctive morphological and ultrastructural features that support this view and suggest its inclusion (at least for now) in a separate novel class.

The first feature is a somewhat peculiar ultrastructure of its somatic dikinetids, which show the presence of the classical root-associated components (i.e. the transverse and postciliary microtubules, plus a kinetodesmal fibre), but also the presence of two additional transverse microtubules in front of triplet 4 of the anterior kinetosome. A single (or more) additional transverse microtubule has also been reported, with different positions, in several other ciliates from various groups besides heterotrichs (Lynn, 2008; da Silva Neto *et al*., 2016). In heterotrichs, usually only one kinetosome is ciliated (Lynn, 2008). For instance, in the armophorean *Parametopidium circumlabens* (Biggar & Wenrich, 1932) Aescht, 1980, a single additional transverse microtubule has been observed in association with somatic dikinetids (da Silva Neto *et al*., 2016). The presence of longitudinal microtubules along the kinetosomes of *Copemetopus mystakophoros* constitutes another feature in common with *Parametopidium* (da Silva Neto *et al*., 2016). In *Copemetopus mystakophoros*, however, any stacking of the flat ribbons formed by the postciliary microtubules has not been observed. This arrangement, constituting a conspicuous fibre called the postciliodesma, typical of Heterotrichea and Karyorelictea, is likewise absent in *Parablepharisma* (Campello-Nunes *et al.*, 2020), which had previously been considered for a long time to belong to Heterotrichea together with *Copemetopus* (Villeneuve-Brachon, 1940; Al-Rasheid, 2001). Thus, the analysis of the fine structure of the somatic kineties does not support the inclusion of *Copemetopus mystakophoros* in the Heterotrichea, in a similar manner to *Parablepharisma* (Campello-Nunes *et al.*, 2020), and does not indicate any specific phylogenetic placement of the genus within Ciliophora. Moreover, owing to the different topology and the lack of ontogenetic studies, at present the dorsal brush of *Copemetopus* cannot be considered homologous to the structure referred to as the dorsal brush of Litostomatea and to the perizonal stripe of Armophorea.

The second feature is the presence of a moustache, a complex arrangement of long, whip-like ciliary units. This peculiar structure does not have homologues in other ciliate classes, although its function is yet to be understood fully.

The third feature is the presence of both mitochondria and hydrogenosome-like structures as energy-related organelles, which has never been described before in ciliates.

The fourth and final feature is the presence in the cytoplasm of many SVs containing two types of bacteria (see Discussion). This feature has been included herein as an additional taxonomic descriptor, according to the current approach suggested for in-depth species characterization (Serra *et al.*, 2020).

All these morphological features form a unique combination supporting the molecular phylogenetic results and suggest that, at least based on current knowledge, *Copemetopus* should be included in a separated novel class of the phylum Ciliophora.

the symbionts of *copemetopus mystakophoros* and other possibly associated prokaryotes

The analysis of the two populations [IPS3-1 (type population) and OALG11] underlined the presence of different species of prokaryotes possibly associated with the ciliate. In the case of the IPS3-1 population, we have a complete dataset, including live observations, FISH and TEM images and molecular data (i.e. 16S rDNA sequences obtained via PCR, cloning and Sanger sequencing). Combining all these data, we consider that the 16S rDNA sequences assigned to OTUs #1 and #2 (i.e. a planctomycetes-like bacterium and a spirochaete bacterium, respectively) might belong to some of the prokaryotes observed in association with *Copemetopus mystakophoros*.

In more detail, we believe that the spirochaete-like bacterium observed in the host symbiontophorous vacuoles could correspond to the OTU #2 sequence. In TEM pictures, spirochaete-like organisms are easily distinguished in such vacuoles (Figs 10E, 12A, B), and it is probable that the two sequences retrieved with the clone library method correspond to the most abundant bacteria associated with the host (i.e. those present in symbiontophorous vacuoles and/or ectosymbionts). Although SEM investigation, which is generally an elective technique in disclosing the presence of ectosymbionts, could not help on this occasion, likely due to procedural issues, the presence of ectosymbionts (Figs 6, 10A) and of a third type of cytoplasmic prokaryote (Fig. 10A) is obvious from both FISH and TEM analyses. Thus, we might hypothesize that one of the two categories could correspond to the OTU #1 sequence.

As a last consideration, we argue that the other type of symbiont present in SVs of *Copemetopus mystakophors* might not have been detected by the clone library method owing to a bias related to the primers that we used, because the ALF1 probe, which showed positive signals for those bacteria, does not fully match the sequences of OTUs #1 and #2.

Concerning the OALG11 population, we analysed the molecular data and the images of living cells to investigate the microbial community possibly associated with *Copemetopus mystakophoros*. The *in vivo* pictures showed the presence of two different morphotypes of prokaryotes included in SVs (Supporting Information, Fig. S4). Moreover, we obtained four 16S rDNA sequences (OTUs #3–#6), different from each other and from those retrieved from the IPS3-1 population. In particular, desulfobacteria were found, namely OTU #4, showing the highest coverage (1466.94×) and probably representing the most numerous prokaryotic organisms associated with *Copemetopus mystakophoros* and, therefore, the most probable candidates to be the true symbionts of the ciliate.

Following the same principle, OTU #5 (‘*Ca.* Cloacimonetes’-like bacterium) would also be a good candidate to be a *Copemetopus* symbiont, given the high coverage (395.71×) and the 16S rDNA low identity percentage after BLAST analysis, which suggests an accelerated evolutionary rate, a common trait in symbiotic prokaryotes (Peek *et al.*, 1998; Itoh *et al.*, 2002). Moreover, little is known about members of ‘*Ca.* Cloacimonetes’, given that no isolates have been characterized fully, except that their sequences have been recovered from anaerobic digesters (Pelletier *et al.*, 2008; Limam *et al.*, 2014) and that they can grow in syntrophy with hydrogenotrophic methanogens (Nobu *et al.*, 2015) and perform the anaerobic digestion of cellulose (Limam *et al.*, 2014).

Syntrophy is defined as a tightly coupled mutualistic interaction between hydrogen-/formate-producing and hydrogen-/formate-using microorganisms (Sieber *et al.*, 2012). We might speculate that syntrophy could also happen in the microniche constituted by *Copemetopus* and its anoxic environment, given that these categories of organisms seem to be associated with the ciliate, such as OTUs #3–#5. Not surprisingly , the symbiosis among ciliates living in anoxic environments and associated prokaryotes that provide physiological advantages in cell respiration is well documented, and it is gaining increasing attention (Embley *et al.*, 1995; Hackstein, 2010; Beinart *et al.*, 2018; Nitla *et al.*, 2019; Graf *et al.*, 2021).

The other two sequences, OTUs #3 and #6, showed a much lower coverage (Table 3), although they belong to groups well known for participating in symbiotic/pathogenic associations, such as Campylobacterota and Archaea (OTU #3 is close to a symbiotic organism: '*Candidatus* Lokiarchaeota archaeon'). Obviously, without further analyses that clarify their association with the host, it is not possible to determine whether OTUs #3–#6 are true symbionts or transitory associated organisms or bacteria present in the food vacuoles. Nevertheless, all the detected sequences belong to prokaryotes not yet described, and this might be a possible suggestion for a symbiotic status.

The fact that two *Copemetopus mystakophoros* populations living in different habitats showed a different composition in their (putative) associated microbial community is not surprising. Many studies have already underlined the possibility for ciliates to retrieve potentially useful prokaryotes from the environment, possibly to replace pre-existing symbionts (Krueger & Cavanaugh, 1997; van Hoek *et al.*, 2000; Vannini *et al.*, 2012; Boscaro *et al.*, 2018; Fokin & Serra, 2022).

The species description of the (putative) symbionts and the analysis of their interaction with the host cell fall outside the aims of the present study and will be a matter of specific future investigation. At present, we can state only that this is a type of obligate symbiosis based on the constant presence of such symbiontophorous vacuoles and their composition in the form of an association of a fairly constant number of bacteria belonging to at least two different morphospecies.

Moreover, it is likely that this feature is also present in other species of the genus and that previous researchers simply did not recognize it or interpret it appropriately. In fact, some of the images provided in these studies, namely figure 19 in the paper by Villeneuve-Brachon (1940) and figure 1 in the paper by Al-Rasheid (2001), showing 'food' vacuoles with uniform-looking, undamaged bacteria might support this hypothesis. Additionally, TEM images from the ciliate referred to as *Copemetopus subsalsus* (Campello-Nunes *et al.*, 2022: fig. 6F) show the presence of bacteria inside cytoplasmatic vacuoles.

TAXONOMY

Copemetopea cl. nov.

Diagnosis:

Body size relatively large; conical in shape, wide anteriorly, tapering posteriorly, with rounded posterior end; cytostome wide at the front, ~50% of body length; macronucleus usually in two equally elongated nodules; micronuclei small, spherical and of the compact type, numerous; in the cytoplasm, numerous slightly elongated symbiontophorous vacuoles carrying bacteria (with two different species); somatic kineties composed of dikinetids, also with some polykinetids (triplets or even up to six kinetids in the same unit); postciliary microtubules well developed, not forming postciliodesma; two sets of transverse microtubules; a row of long, whip-like ciliary units (moustache) inserted on an outer border of the buccal cavity over oral polykinetids, without any connection with them; dorsal brush consisting of dense rows of longer somatic cilia beneath the

anterior cell pole, on the right side; left serial oral polykinetids looking like a classical AZM; paroral infraciliature as a long row of kinetosomal triplets; from anoxic brackish water to marine sediments; one order: Copemetopida.

Copemetopida ord. nov.

With characters of the class; one family: Copemetopidae.

Copemetopidae fam. nov.

With characters of the class; one genus: *Copemetopus*.

Copemetopus Villeneuve-Brachon, 1940

Type locality:

Saline ponds off the French coast of the Mediterranean Sea near Sète ('Fossé de la route de Sète à Agde'; Villeneuve-Brachon, 1940).

Type species:

Copemetopus subsalsus Villeneuve-Brachon, 1940. Typification by Villeneuve-Brachon (1940) by monotypy (see also Aescht, 2001).

Etymology:

No etymology of the name *Copemetopus* has been provided concomitantly with the establishment of the genus by Villeneuve-Brachon (1940). Etymology of new names is only recommended (Recommendation 25C of the International Commission on Zoological Nomenclature, 1999). [Editorial note: It might be derived from the Greek κωπη, club or oar, and the ciliate genus *Metopus*].

Amended diagnosis:

Body size from medium to large (120–450 µm); non-contractile; conical shape: wide anteriorly, tapering posteriorly; oral aperture (cytostome) wide at the front, ~50% of body length; macronucleus usually in two equally elongated nodules with a thin, not always visible isthmus in between; micronuclei small, spherical, numerous. Contractile vacuole not detected for all the species; cytoproct not visible; in the cytoplasm of some species, numerous slightly elongated symbiontophorous vacuoles carrying bacteria (two different types); somatic kineties mainly present as rows of dikinetids with all kinetosomes ciliophorous, also with some triplets or even up to six kinetids in the same unit; postciliary microtubules well developed, not forming postciliodesma; two sets of transverse microtubules; a row of long, whip-like ciliary units (moustache) inserted on an outer border of the buccal cavity over AZM polykinetids, without any connection with them; they have a restricted motility and do not participate in the function of AZM; dorsal brush consisting of dense rows of longer somatic cilia beneath the anterior cell pole, on the right side; left serial oral polykinetids look like as a classical AZM; paroral infraciliature as a long row of kinetosomal triplets/doublets; from anoxic brackish water to marine or hypersaline sediments (15–130‰). Until now, including at least five species:

- *Copemetopus subsalsus* Villeneuve-Brachon, 1940 (type species),
- *Copemetopus subsalsus sensu* Al-Rasheid (2001),
- *Copemetopus chesapeakensis* Small & Lynn, 1985,
- *Copemetopus verae* Campello-Nunes *et al.*, 2022
- *Copemetopus mystakophoros* sp. nov.

Remarks:

Copemetopus mystakophoros, described herein, is the only species of the genus for which both deposited slides defining the holotype and paratype (i.e. voucher material) and a complete set of data (i.e. morphological, ultrastructural and molecular data) useful for species identification are available so far.

DATA AVAILABILITY STATEMENT

The data that support the findings of this study are openly available in free access on-line repository or are available from the authors upon reasonable request.

ACKNOWLEDGEMENTS

Special acknowledgements to Simone Gabrielli for tree and photograph-editing support. We also thank the Editor, Maarten Christenhusz, for constructive comments on this manuscript. This work was supported by the University of Pisa (project PRA_2018_63); the research leading to these results has received funding from the European Community's H2020 Programme H2020-MSCA-RISE 2019, under grant agreement no. 872767. The present study was also supported by the Fondazione Cassa di Risparmio di Pistoia e Pescia, giovani@ricercascientifica2019 fellowship (no. 2019.0380).

CONFLICTS OF INTEREST

Authors declare that they do not have any conflict of interest.

REFERENCES

Aescht E. 2001. Catalogue of the generic names of ciliates (Protozoa, Ciliophora). *Denisia* **1**: 1–350.

Agatha S, **Ganser MH**, **Santoferrara LF. 2021**. The importance of type species and their correct identification: a key example from tintinnid ciliates (Alveolata, Ciliophora, Spirotricha). *Journal of Eukaryotic Microbiology* **68**: e12865.

Al-Rasheid KAS. 2001. Redescription of the rare heterotrichid ciliate, *Copemetopus subsalsus* Villeneuve-Brachon, 1940. *Journal of Eukaryotic Microbiology* **48**: 188–193.

Amann RI, **Binder BJ**, **Olson RJ**, **Chisholm SW**, **Devereux R**, **Stahl D. 1990**. Combination of 16S rRNA-targeted oligonucleotide probes with flow cytometry for analyzing mixed microbial populations. *Applied and Environmental Microbiology* **56**: 1919–1925.

Bankevich A, **Nurk S**, **Antipov D**, **Gurevich AA**, **Dvorkin M**, **Kulikov AS**, **Lesin VM**, **Nikolenko SI**, **Pham S**, **Prjibelski AD**, **Pyshkin AV**, **Sirotkin AV**, **Vyahhi N**, **Tesler G**, **Alekseyev MA**, **Pyshkin AV. 2012**. SPAdes: a new genome assembly algorithm and its applications to single-cell sequencing. *Journal of Computational Biology* **19**: 455–477.

Beinart RA, **Beaudoin DJ**, **Bernhard JM**, **Edgcomb VP. 2018**. Insights into the metabolic functioning of a multipartner ciliate symbiosis from oxygen-depleted sediments. *Molecular Ecology* **27**: 1794–1807.

Boscaro V, **Carducci D**, **Barbieri G**, **Senra MVX**, **Andreoli I**, **Erra F**, **Petroni G**, **Verni F**, **Fokin SI. 2014**. Focusing on genera to improve species identification: revised systematics of the ciliate *Spirostomum*. *Protist* **165**: 527–541.

Boscaro V, **Fokin SI**, **Petroni G**, **Verni F**, **Keeling PJ**, **Vannini C. 2018**. Symbiont replacement between bacteria of different classes reveals additional layers of complexity in the evolution of symbiosis in the ciliate *Euplotes*. *Protist* **169**: 43–52.

Buonanno F, **Ortenzi C. 2018**. Predator-prey interactions in ciliated protists. In: Najjari A, Cherif A, Sghaier H, Ouzari HI, eds. *Extremophilic microbes and metabolites – diversity, bioprospecting and biotechnological applications*. London: InTechOpen, 13–40.

Campello-Nunes PH, **Fernandes NM**, **Szokoli F**, **Fokin SI**, **Serra V**, **Modeo L**, **Petroni G**, **Soares CAG**, **da Silva Paiva T**, **da Silva-Neto ID. 2020**. *Parablepharisma* (Ciliophora) is not a heterotrich: a phylogenetic and morphological study with the proposal of new taxa. *Protist* **171**: 125716.

Campello-Nunes PH, da **Silva-Neto ID**, **Sales MH**, **Soares CA**, **da Silva Paiva T**, **Fernandes NM. 2022**. Morphological and phylogenetic investigations shed light on evolutionary relationships of the enigmatic genus *Copemetopus* (Ciliophora, Alveolata), with the proposal of *Copemetopus verae* sp. nov. *European Journal of Protistology* **83**: 125878.

Corliss JO. 1953. Silver impregnation of ciliated protozoa by the Chatton-Lwoff technic. *Stain Technology* **28**: 97–100.

Corliss JO. 1979. *The ciliated protozoa: characterization, classification, and guide to the literature* (2nd ed., 455 pp.). London/New York: Pergamon Press.

Darriba D, **Taboada GL**, **Doallo R**, **Posada D. 2011**. ProtTest 3: fast selection of best-fit models of protein evolution. *Bioinformatics* **27**: 1164–1165.

Embley TM, **Finlay BJ**, **Dyal PL**, **Hirt RP**, **Wilkinson M**, **Williams AG. 1995**. Multiple origins of anaerobic ciliates with hydrogenosomes within the radiation of aerobic ciliates. *Proceedings of the Royal Society B: Biological Sciences* **262**: 87–93.

Esteban G, **Fenchel T**, **Finlay B. 1995**. Diversity of free- living morphospecies in the ciliate genus *Metopus*. *Archiv für Protistenkunde* **146**: 137–164.

Fernandes NM, **Vizzoni VF**, **Borges BDN**, **Soares CAG**, **da Silva-Neto ID**, **da Silva Paiva T. 2018**. Molecular phylogeny and comparative morphology indicate that odontostomatids (Alveolata, Ciliophora) form a distinct class-level taxon related to Armophorea. *Molecular Phylogenetics and Evolution* **126**: 382–389.

Foissner W. 1993. *Colpodea (Ciliophora)*. Stuttgart, Jena, New York: Gustav Fisher.

Fokin SI. 2016. FISH technique as a possible tool for cortex investigation in armophorean ciliates (Ciliophora, Armophorea). *Protistology* **10**: 19.

Fokin SI, **Ferrantini F**, **Modeo L**, **Verni F**, **Petroni G. 2009**. *Copemetopus subsalsus*, *Parablepharisma bacteriophora* and a new *Parablepharisma*-like organism from habitats with oxygen deficiency – are they heterotrichs? Abstracts of 28 Wissenschaftliche Jahrestagung der Deutschen Gesellschaft für Protozoologie, 18.

Fokin S, **Görtz H-D. 1993**. *Caedibacter macronucleorum* sp. nov., a bacterium inhabiting the macronucleus of *Paramecium duboscqui*. *Archiv für Protistenkunde* **143**: 319–324.

Fokin SI, **Modeo L**, **Andreoli I**, **Ferrantini F**, **Vannini C**, **Rosati G**, **Verni F**, **Petroni G. 2006**. Rare specie di ciliati raccolti in Toscana in ambienti salmastri microaerofili. 67 Congresso Nazionale Unione Zoologica Italiana. Napoli, 12–15 September, 79–80.

Fokin SI, **Modeo L**, **Andreoli I**, **Ferrantini F**, **Verni F**, **Petroni G. 2008**. Some rare ciliate species of *Copemetopus*, *Parablepharisma* and *Sonderia* genera (Ciliophora, Protista) revealed from brackish water habitats with oxygen deficiency in Tuscany, Italy. Abstracts from the XX International Congress of Zoology, Paris, August. *Integrative Zoology* **31**: 26–29.

Fokin SI, **Serra V. 2022**. Bacterial symbiosis in ciliates (Alveolata, Ciliophora): roads travelled and those still to be taken. *Journal of Eukaryotic Microbiology* **69**: e12886.

Fokin SI, **Serra V**, **Andreoli I**, **Verni F**, **Petroni G**, **Modeo L. 2019**. *Copemetopus mystakophoros* sp. nov. a new representative of the ciliate genus from brackish water pond on Ligurian sea coastline (Tuscany, Italy). VIII European Congress of Protistology–ISOP joint meeting. Rome, Italy, 28 July–2 August 2019. *Book of Abstracts*, 178.

Graf JS, **Schorn S**, **Kitzinger K**, **Ahmerkamp S**, **Woehle C**, **Huettel B**, **Schubert CJ**, **Kuypers MMM**, **Milucka J. 2021**. Anaerobic endosymbiont generates energy for ciliate host by denitrification. *Nature* **591**: 445–450.

Guindon S, **Gascuel O. 2003**. A simple, fast, and accurate algorithm to estimate large phylogenies by maximum likelihood. *Systematic Biology* **52**: 696–704.

Hackstein JHP. 2010. Anaerobic ciliates and their methanogenic endosymbionts. In: Hackstein JHP, ed. *(Endo)symbiotic methanogenic Archaea. Microbiology monographs.* Berlin, Hiedelberg: Springer-Verlag **19**: 13–23.

van Hoek AHAM, **van Alen TA**, **Sprakel VSI**, **Leunissen JAM**, **Brigge T**, **Vogels GD**, **Hackstein JHP. 2000**. Multiple acquisition of methanogenic archaeal symbionts by anaerobic ciliates. *Molecular Biology and Evolution* **17**: 251–258.

Iftode F, **Fryd-Versavel G**, **Curgy JJ. 1982**. *Copemetopus* Villeneuve Branchon, 1940, Condylostomidé mal connu et original. Comparaison avec d'autres hétérotriches et avec des ciliés dits anaérobies. *Journal of Protozoology* **29**: 518.

International Commission on Zoological Nomenclature. 1999. In: **Ride WDL**, **Cogger HG**, **Dupuis C**, **Kraus O**, **Minelli A**, **Thompson FC**, **Tubbs PK**, eds. *International code of zoological nomenclature*. London: International Trust for Zoological Nomenclature. Chapter 7, Article 25, https://code.iczn.org/formation-and-treatment-of-names/ article-25-formation-and-treatment-of-names/?frame=1

Itoh T, **Martin W**, **Nei M. 2002**. Acceleration of genomic evolution caused by enhanced mutation rate in endocellular symbionts. *Proceedings of the National Academy of Sciences of the United States of America* **99**: 12944–12948.

Jankowsky AV. 2007. Phylum Ciliophora Doflein, 1901. Review of taxa. In: *Handbook on zoology. Protista. Part 2*. St. Petersburg: Nauka, 415–993 [in Russian with English summary].

Krueger DM, **Cavanaugh CM. 1997**. Phylogenetic diversity of bacterial symbionts of Solemya hosts based on comparative sequence analysis of 16S rRNA genes. *Applied and Environmental Microbiology* **63**: 91–98.

Limam RD, **Chouari R**, **Mazeas L**, **Wu TD**, **Li T**, **Grossin- Debattista J**, **Guerquin-Kern J-L**, **Saidi M**, **Landoulsi A**, **Sghir A**, **Bouchez T. 2014**. Members of the uncultured bacterial candidate division WWE 1 are implicated in anaerobic digestion of cellulose. *Microbiology Open* **3**: 157–167.

Lynn DH. 2008. *The ciliated Protozoa: characterization, classification, and guide to the literature*. Guelph: University of Guelph.

Lynn DH, **Corliss JO. 1991**. Ciliophora. In: *Microscopic anatomy of invertebrates. 1 Protozoa.* New York: Wiley-Liss, Inc., 333–467.

Lynn DH, **Small EB. 2002**. Phylum Ciliophora Doflein, 1901. In J. J. Lee, G. F. Leedale, & P. C. Bradbury (Eds.), *An illustrated guide to the protozoa* Vol. **1** (**2000**). Kansas, USA: Society of Protozoologists, Lawrence, pp. 371–656.

Manz W, **Amann R**, **Ludwig W**, **Wagner M**, **Schleifer KH. 1992**. Phylogenetic oligodeoxynucleotide probes for the major subclasses of proteobacteria: problems and solutions. *Systematic and Applied Microbiology* **15**: 593–600.

Medlin L, **Elwood HJ**, **Stickel S**, **Sogin ML. 1988**. The characterization of enzymatically amplified eukaryotic 16S-like rRNA-coding regions. *Gene* **71**: 491–499.

Mironova EI, **Telesh IV**, **Skarlato SO. 2009**. Planktonic ciliates of the Baltic Sea (a review). *Inland Water Biology* **2**: 13–24.

Modeo L, **Fokin SI**, **Boscaro V**, **Andreoli I**, **Ferrantini F**, **Rosati G**, **Verni F**, **Petroni G. 2013**. Morphology, ultrastructure, and molecular phylogeny of the ciliate *Sonderia vorax* with insights into the systematics of order Plagiopylida. *BMC Microbiology* **13**: 401–423.

Modeo L, **Rosati G**, **Andreoli I**, **Gabrielli S**, **Verni F**, **Petroni G. 2006**. Molecular systematics and ultrastructural characterization of a forgotten species: *Chattonidium setense* (Ciliophora, Heterotrichea). *Proceedings of the Japan Academy, Series B* **82**: 359–374.

Nitla V, **Serra V**, **Fokin SI**, **Modeo L**, **Verni F**, **Sandeep BV**, **Kalavati C**, **Petroni G. 2019**. Critical revision of the family *Plagiopylidae* (Ciliophora: Plagiopylea), including the description of two novel species, *Plagiopyla ramani* and *Plagiopyla narasimhamurtii*, and redescription of *Plagiopyla nasuta* Stein, 1860 from India. *Zoological Journal of the Linnean Society* **186**: 1–45.

Nobu MK, **Narihiro T**, **Rinke C**, **Kamagata Y**, **Tringe SG**, **Woyke T**, **Liu WT. 2015**. Microbial dark matter ecogenomics reveals complex synergistic networks in a methanogenic bioreactor. *The ISME Journal* **9**: 1710–1722.

Oren A, **Garrity GM. 2021**. Valid publication of the names of forty-two phyla of prokaryotes. *International Journal of Systematic and Evolutionary Microbiology* **71**: 005056.

Orsi W, **Edgcomb V**, **Faria J**, **Foissner W**, **Fowle WH**, **Hohmann T**, **Suarez P**, **Taylor C**, **Taylor GT**, Vďačný **P**, **Epstein SS. 2012**. Class Cariacotrichea, a novel ciliate taxon from the anoxic Cariaco Basin, Venezuela. *International Journal of Systematic and Evolutionary Microbiology* **62**: 1425–1433.

Peek AS, **Vrijenhoek RC**, **Gaut BS. 1998**. Accelerated evolutionary rate in sulfur-oxidizing endosymbiotic bacteria associated with the mode of symbiont transmission. *Molecular Biology and Evolution* **15**: 1514–1523.

Pelletier E, **Kreimeyer A**, **Bocs S**, **Rouy Z**, **Gyapay G**, **Chouari R**, **Rivière D**, **Ganesan A**, **Daegelen P**, **Sghir A**, **Cohen GN**, **Médigue C**, **Weissenbach J**, **Le Paslier D. 2008**. '*Candidatus* Cloacamonas acidaminovorans': genome sequence reconstruction provides a first glimpse of a new bacterial division. *Journal of Bacteriology* **190**: 2572–2579.

Petroni G, **Dini F**, **Verni F**, **Rosati G. 2002**. A molecular approach to the tangled intrageneric relationships underlying phylogeny in *Euplotes* (Ciliophora, Spirotrichea). *Molecular Phylogenetics and Evolution* **22**: 118–130.

Quast C, **Pruesse E**, **Yilmaz P**, **Gerken J**, **Schweer T**, **Yarza P**, **Peplies J**, **Glöckner FO. 2013**. The SILVA ribosomal RNA gene database project: improved data processing and web-based tools. *Nucleic Acids Research* **41**: D590–D596.

Ronquist F, **Teslenko M**, **Van Der Mark P**, **Ayres DL**, **Darling A**, **Höhna S**, **Larget B**, **Liu L**, **Suchard MA**, **Huelsenbeck JP. 2012**. MrBayes 3.2: efficient Bayesian phylogenetic inference and model choice across a large model space. *Systematic Biology* **61**: 539–542.

Rosati G, **Modeo L. 2003**. Extrusomes in ciliates: diversification, distribution, and phylogenetic implications. *Journal of Eukaryotic Microbiology* **50**: 383–402.

Rosati G, **Modeo L**, **Melai M**, **Petroni G**, **Verni F. 2004**. A multidisciplinary approach to describe protists: a morphological, ultrastructural, and molecular study on *Peritromus kahli* (Ciliophora, Heterotrichea). *Journal of Eukaryotic Microbiology* **51**: 49–59.

Rotterová J, **Salomaki E**, **Pánek T**, **Bourland W**, **Žihala D**, **Táborský P**, **Edgcomb VP**, **Beinart RA**, **Kolísko M**, **Čepička I. 2020**. Genomics of new ciliate lineages provides insight into the evolution of obligate anaerobiosis. *Current Biology* **30**: 2037–2050.e6.

Seemann T. 2013. *Barrnap 0.8: rapid ribosomal RNA prediction*. Available at: https://github.com/tseemann/ barrnap. (date last accessed 2 March 2023).

Serra V, **Gammuto L**, **Nitla V**, **Castelli M**, **Lanzoni O**, **Sassera D**, **Bandi C**, **Sandeep BV**, **Verni F**, **Modeo L**, **Petroni G. 2020**. Morphology, ultrastructure, genomics, and phylogeny of *Euplotes vanleeuwenhoeki* sp. nov. and its ultra- reduced endosymbiont '*Candidatus* Pinguicoccus supinus' sp. nov. *Scientific Reports* **10**: 20311.

Sieber JR, **McInerney MJ**, **Gunsalus RP. 2012**. Genomic insights into syntrophy: the paradigm for anaerobic metabolic cooperation. *Annual Review of Microbiology* **66**: 429–452.

da Silva-Neto ID, **Grolière CA**, **Puytorac P**, **Chaouite J. 1993**. Observations sur la structure et l'ultrastructure de *Copemetopus* sp., cilie heterotrichida. *Journal of Protozoology* **40**: 37A.

da Silva-Neto ID, **da Silva Paiva T**, **do Nascimento Borges B**, **Harada ML. 2016**. Fine structure and molecular phylogeny of *Parametopidium circumlabens* (Ciliophora: Armophorea), endocommensal of sea urchins. *Journal of Eukaryotic Microbiology* **63**: 46–61.

Skovorodkin IN. 1990. A device for immobilization of small biological objects during light microscopical observation. *Tsitologia* **32**: 87–91 [in Russian with English summary].

Small EB, **Lynn DH. 1985**. Phylum Ciliophora. In: Lee JJ, Hutner SH., Bovee EC eds. *An illustrated guide to the Protozoa*. Lawrence: Allen Press, 393–575.

Vannini C, **Ferrantini F**, **Ristori A**, **Verni F**, **Petroni G. 2012**. *Betaproteobacterial* symbionts of the ciliate *Euplotes*: origin and tangled evolutionary path of an obligate microbial association. *Environmental Microbiology* **14**: 2553–2563.

Villeneuve-Brachon S. 1940. Recherches sur les ciliés hétérotriches. Cinétome, argyrome, myonémes. *Archives de Zoologie Expérimentale et Générale* **82**: 1–180.

Warren A, **Patterson DJ**, **Dunthorn M**, **Clamp JC**, **Achilles-Day UE**, **Aescht E**, **Al-Farraj SA**, **Al-Quraishy S**, **Al-Rasheid K**, **Carr M**, **Day JG**, **Dellinger M**, **El-Serehy HA**, **Fan Y**, **Gao F**, **Gao S**, **Gong J**, **Gupta R**, **Hu X**, **Kamra K**, **Langlois G**, **Lin X**, **Lipscomb D**, **Lobban CS**, **Luporini P**, **Lynn DH**, **Ma H**, **Macek M**, **Mackenzie-Dodds J**, **Makhija S**, **Mansergh RI**, **Martín- Cereceda M**, **McMiller N**, **Montagnes DJS**, **Nikolaeva S**, **Ong'ondo GO**, **Pérez-Uz B**, **Purushothaman J**, **Quintela-Alonso P**, **Rotterová J**, **Santoferrara L**, **Shao C**, **Shen Z**, **Shi X**, **Song W**, **Stoeck T**, **La Terza A**, **Vallesi A**, **Wang M**, **Weisse T**, **Wiackowski K**, **Wu L**, **Xu K**, **Yi Z**, **Zufall R**, **Agatha S. 2017**. Beyond the 'Code': a guide to the description and documentation of biodiversity in ciliated protists (Alveolata, Ciliophora). *Journal of Eukaryotic Microbiology* **64**: 539–554.

Westram R, **Bader K**, **Pruesse E**, **Kumar Y**, **Meier H**, **Glöckner FO**, **Ludwig W. 2011**. ARB: a software environment for sequence data. In: De Bruijn FJ, ed. *Handbook of molecular microbial ecology I: metagenomics and complementary approaches*. London: Wiley-Blackwell, 399–406.

Xu K, **Agatha S**, **Dolan J. 2021**. World Ciliophora Database. *Copemetopus* Villeneuve-Brachon, 1940. Accessed through: World Register of Marine Species. Available at: http://www.marinespecies.org/aphia.php?p=taxdetails&id=425686 (date last accessed 12 October 202/1).